

A framework for ground-up life cycle assessment of novel, carbon-storing building materials

Seth Kane ^{a,†}, Baishakhi Bose ^b, Thomas P. Hendrickson ^c, Jin Fan ^a, Sarah L. Nordahl ^c, Corinne D. Scown ^{b,c,d,e}, Sabbie A. Miller ^a

^a Department of Civil and Environmental Engineering, University of California, Davis

^b Biological Systems and Engineering Division, Lawrence Berkeley National Laboratory

^c Energy Analysis and Environmental Impacts Division, Lawrence Berkeley National Laboratory

^d Joint BioEnergy Institute, Lawrence Berkeley National Lab

^e Energy & Biosciences Institute, University of California, Berkeley

[†] Corresponding Author: T +1 907 750 6364, E skane@ucdavis.edu

Abstract:

Currently, materials production is responsible for over 25% of anthropogenic CO₂ emissions. However, due to their long-lived nature and enormous scale of production, some building materials offer a potential means for atmospheric carbon storage. Accurate emissions accounting is key to understanding this potential, yet life-cycle inventory (LCI) databases struggle to keep up with the wide array of novel materials and provide the data to accurately characterize their effect on net carbon dioxide equivalent (CO₂e) emissions and uptake. To this end, we offer a framework for developing LCIs from the ground up using thermodynamic first principles and provide guidance on alternative approaches to characterize material LCIs from limited data when first principles approaches are not feasible. This framework provides a generalizable methodology to develop and compare LCIs of novel material production. To ensure the accuracy of this framework and provide step-by-step examples of its application, we consider the following mineral-based and bio-based building materials: Portland cement, low-carbon steel, gypsum board, and cross-laminated timber from yellow poplar and eastern hemlock, showing good agreement with existing LCIs. This framework is developed with a particular focus on describing CO₂e emissions and energy consumption of material production, but could be extended to other environmental impacts or applications. Grounding initial LCIs in first principles can guide the early-stage design of novel materials and processes to minimize CO₂e emissions or improve the carbon sequestration potential of critical materials across sectors.

Keywords:

Carbon uptake; carbon sequestration; carbon dioxide removal; life-cycle inventory; industrial decarbonization

1. Introduction

Materials production accounts for approximately 25% of global anthropogenic greenhouse gas (GHG) emissions.^{1,2} Building materials are particularly important, contributing nearly two-thirds of material emissions, and 39 Gt of building materials were produced and used globally in 2019.¹ Several groups, including the National Academies of Science, Engineering, and Medicine, have argued that building materials are particularly well suited to act as carbon dioxide removal (CDR) or carbon utilization systems due to their immense scale of production and long-lived applications,³ and studies suggest up to 16.6 Gt of CO₂ could be stored in building materials annually.⁴ However, to achieve carbon storage in building materials, rapid development and growth in novel materials for buildings and energy are required.^{5,6} Accurate accounting of emission fluxes associated with the production of novel materials is needed to ensure carbon removal is achieved, and such data is challenging to accurately assess at early technology readiness levels (TRLs). Therefore, to capitalize on material carbon storage potential, systemic accounting of material production emissions at low TRLs and with poor data availability is needed.

To ensure novel materials are low-emission or carbon-negative, their GHG emissions must be quantified, but life cycle assessments (LCA) of novel materials and processes are challenging due to inherent inventory data limitations.⁷⁻⁹ Due to the data-poor environment of novel materials production, life cycle inventory (LCI) data often must be extrapolated from similar processes or laboratory-scale experiments, leading to increased uncertainty in emissions and challenges in comparing the life cycle emissions of novel materials.¹⁰ A true apples-to-apples comparison of novel processes to an existing, commercial-scale operation is inappropriate when LCI data for novel processes only reflects laboratory or pilot-scale activities while high-quality, commercial data characterizes the existing technology.⁸ Furthermore, methods of estimating LCI data are often not standardized between studies, with past studies taking an individualized approach to the production processes they consider, which may not accurately model other material production processes. Such methodology differences make the comparison of results between studies that use different modeling methods and assumptions challenging.¹¹ Proposed methods to estimate LCIs when data are limited include proxy selection, development of machine learning models, chemical process simulation, or estimation based on the thermodynamic and chemical first principles of material synthesis.⁹ Past studies have shown that these methods have a fundamental tradeoff between data accuracy and data requirements, with specific-process data for a single facility being the most accurate but also requiring costly data collection, while proxy selection is the least accurate.¹⁰ When new technologies are early in the research and development process (e.g., lab-scale), estimations from first principles and thermodynamics may be the most accurate method to estimate LCI data with existing process data collected. Development of a systematic methodology that assesses the LCI of novel processes step-by-step, accounting for key material production processes from the ground up and with first principles approaches, would minimize the reduced accuracy of estimating LCIs at early development stages. Creating a standardized framework to determine such data could allow accurate comparisons between LCIs for novel materials to inform policy and development decisions surrounding industrial decarbonization.

To overcome data challenges with LCA, a ground-up, first-principles approach can simplify LCI data acquisition while focusing on the core processes in material production. A first-principles approach is considered a critical approach to estimating LCI data. It could be well suited for products reliant on chemical conversion for the production of key mineral or fossil-derived materials, such as cement, metals, or plastics. Such approaches have previously been applied to examine novel pathways to produce key chemicals while reconciling mass and energy balances,¹² to examine alternative cement

1 chemistries with a directly comparable methodological approach,¹³ and to compare different methods of
2 estimating LCI data for key materials.¹⁰ For some process steps, such as growth and harvesting of
3 biogenic resources or mining of minerals, a first principles thermodynamic approach would be
4 extremely challenging to capture complex factors, such as biomass growth and resource requirements,
5 and first principles alone will not suffice in building out a comprehensive LCI. In these cases, a limited
6 first-principles approach can be combined with a ground-up approach to individually assess each
7 element of the product life cycle. Pairing this ground-up approach with a first-principles approach when
8 appropriate can help isolate data challenges in the life cycle to address and minimize uncertainties while
9 maximizing accuracy for life-cycle stages where high-quality data are available. A combined first-
10 principles approach to model conversion processes and a ground-up approach to model other process
11 steps, such as resource extraction, could address data gaps in first-principles-only LCI estimation
12 methods. However, there is a need for a systematic methodological framework that can be broadly
13 applied to materials production to create accurate and consistent LCIs for novel materials in data-limited
14 environments.

15
16 This work presents a systematic framework for assessing cradle-to-gate material environmental impacts
17 with a ground-up approach. While this framework could be applied to develop complete LCIs, herein,
18 we focus on GHG emissions and energy consumption, given the critical role these impact categories
19 play in CDR and decarbonization efforts. This framework is developed step-by-step to provide crucial
20 aid in developing LCIs for novel, carbon-storing building materials, given the urgent need to develop
21 methods to decarbonize and store carbon in the built environment. However, this framework is
22 generalizable and can also be applied to materials in other critical sectors, including, but not limited to,
23 materials for renewable energy, battery materials, and biofuels. The developed framework is applied to
24 and validated for conventional building materials from both mineral and biogenic resources to
25 demonstrate the integration of the ground-up and first-principles components. This developed
26 framework fills a critical need for a systematic method for determining novel materials' life cycle
27 inventories and bridges data accuracy gaps between first-principle calculations and full process
28 simulation.

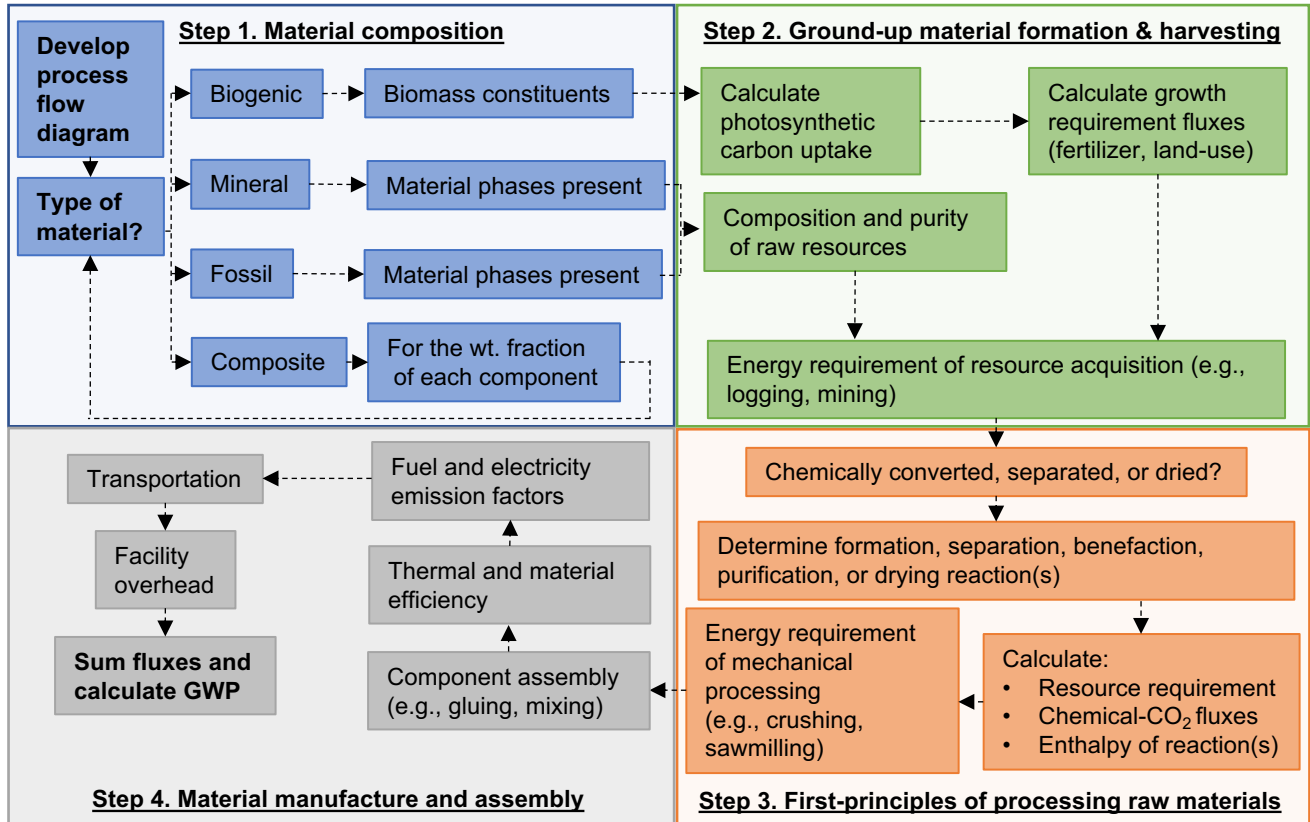
30 **2. Methods**

31 **2.1 Analysis Framework**

32 The developed framework (Figure 1) is broadly applicable to the production of materials and chemicals.
33 In this framework, we pair a ground-up approach to assess processes where estimating data from first
34 principles would be challenging (e.g., biomass growth and harvesting, mining, or mechanical
35 processing) with a first-principles approach to estimating the LCI of chemical processing and
36 conversion. By breaking down material production into individual process steps, this framework allows
37 for higher quality LCI data to be selected for any individual sub-process if available. The ground-up
38 approach allows for the consideration of the role of individual process parameters on LCIs, based on
39 existing data, to allow for a more robust estimation of these processes than proxy selection would
40 provide.

41
42 Herein, we focus on two primary material categories: biogenic and mineral-derived materials, given the
43 critical role these material types play in the construction industry and their broad potential for carbon
44 storage. The modeling approach taken for these material types primarily differs in the accounting of
45 material formation and harvesting (Sec. 2.1.2) processes, such as forestry and agricultural processes for

1 biogenic materials and mining for mineral-derived materials. While chemical conversion processes are
 2 more relevant for mineral-derived material production, a similar approach could be taken for the
 3 chemical processing of biomass. This framework could be adapted to other material classes (e.g., fossil-
 4 derived materials or chemicals, composite materials of multiple categories) by pairing a ground-up
 5 approach to resource acquisition specific to the raw resources used with a first-principles approach to
 6 material processing and conversion. Composite materials can be considered a sum of their components,
 7 with component assembly considered in Step 4, and combined materials can be modeled either
 8 individually with the ground-up approach developed herein or by relying on existing LCIs. The
 9 following subsections correspond to the steps of the framework shown in Figure 1.



11
 12 **Figure 1.** High-level flow diagram of the developed framework for biogenic, mineral-derived, fossil-derived, and composite
 13 materials.
 14

15 **2.1.1 Material Composition**

16 Detailed knowledge of material phase composition is critical to the determination of the formation
 17 reactions of material phases and raw resource requirements before any formation reactions. For biogenic
 18 materials, this includes the composition of constituent biomass phases (e.g., cellulose, lignin, moisture,
 19 and carbon content) to inform modeling inputs and outputs throughout the material life cycle. For
 20 example, as tabulated in Supplemental Table 1 and 2, specific biomass species will have composition
 21 variations depending on growing methods and regions that will impact carbon fluxes, processing
 22 requirements, performance in use, and final potential for reuse and recovery. Additionally, at this stage,
 23 a process flow diagram for material production (e.g., Figure 2 or 3, Supplemental Figures 1 or 2) should
 24 be produced to aid in the determination of process parameters for future steps, and a system boundary
 25 should be determined.

26 **2.1.2 Raw material formation and harvesting**
 27

1 A ground-up approach is taken to material harvesting processes, such as biomass growth and mining.
2 First, the composition of the raw material is determined, such as mineral phases present (e.g., calcite,
3 silica, hematite in common mineral resources) or biogenic constituents (e.g., cellulose, hemicellulose,
4 lignin, ash, and moisture content). This analysis can rely on previously reported literature values as is
5 done herein for mineral resources (see Section 2.3), but similar approaches can be used with site-specific
6 mineralogy information, biogenic resource composition, or composition of fossil feedstocks.

7
8 For biogenic materials, growth and harvesting resources will vary by species, material composition, and
9 growing region. Differences in determining carbon stored in growth will meaningfully affect overall
10 life-cycle impacts. Carbon fluxes in plant growth can be highly uncertain and sensitive to a number of
11 variables, including local climate, soil conditions and composition, nutrient availability, and other
12 factors.¹⁷ Identifying accurate estimates for carbon storage can be challenging, and for our framework
13 application (see Section 2.3), we utilized existing literature for a specific region and lumber species.
14 Other biogenic carbon literature and databases, such as the recent Roads to Removal Forest Carbon
15 Storage model,¹⁷ can be helpful in generating carbon storage estimates. For cultivated biomass that
16 requires fertilizer application, nitrogen inputs are a key driver of GHG emissions, both because of the
17 energy-intensive production and because several percent of applied nitrogen is subsequently emitted as
18 N₂O. Nitrogen inputs can be estimated based on the biomass composition, the amount needed to replace
19 what is harvested and removed from land, and approximated nitrogen use efficiency values.¹⁸

20
21 Additionally, for biogenic materials, other inputs and resource requirements for crop cultivation and
22 harvest need to be considered in capturing life-cycle impacts, but they do not typically incorporate a first
23 principles approach, as we expect LCI data to be readily available. This includes material inputs such as
24 herbicides, insecticides, and fuel use in harvest equipment, which should be obtained from relevant
25 models (e.g., the GHGs, Regulated Emissions, and Energy use in Technologies [GREET] model¹⁹),
26 existing LCI data, and literature for specific biomass species and locations.

27
28 Notably, biomass cultivation also involves carbon uptake during biomass growth. To calculate the CO₂
29 equivalent stored in the final product (e.g., CLT), a carbon content of 50% of the total wood was used.
30 Similarly to the stoichiometric balance calculations for minerals, we modeled CO₂ uptake as 3.67 times
31 the carbon content. Cradle-to-gate GHG emissions presented in subsequent discussions are shown, both
32 excluding and including biogenic CO₂, to perform a harmonized validation comparison with past studies.

33
34 For logging and other agricultural harvesting processes, refinement of the LCI based on location is
35 critical, as logging operations will differ depending on the type(s) of forest and local topology, including
36 slope. This not only impacts energy demand for logging and transportation but also the expected
37 biomass availability in a given year, tied to sustainable removal rates.

38
39 For mining and fossil extraction processes, robust LCIs exist for current mining resources and extraction
40 methods, which can be leveraged for processes that utilize existing mineral resources in novel materials
41 or processes. In these cases, emissions from mining can be evaluated using existing LCI data (e.g., from
42 ecoinvent²⁰ or the US LCI database²¹) associated with mining, quarrying, and extraction of these
43 resources. However, even for well-established mineral extraction methods, there is meaningful spatial
44 variation in the purity, extraction depth, mining method used, etc., which is expected to result in
45 variation in emissions associated with mining and fossil extraction processes. For novel mineral
46 extraction processes, emissions should be estimated using a ground-up approach based on data for
47 similar extraction methods, depth, hardness, and mineral composition.

2.1.3 Processing and conversion of raw materials

The analysis of material formation and procurement differs for materials that are chemically converted or separated during processing compared to those that are not. For materials that undergo chemical transformation or separation (e.g., common mineral-derived materials or biorefineries), the initial step of this stage is the determination of the chemical reactions required to form the final material from raw material resources. Based on the formation reactions, the following are determined:

1. The stoichiometrically required raw material phases are determined from the chemical reaction based on the molar ratios of feedstocks to products and the relative molecular weights. Based on these values and the raw material composition determined in Step 1, the mass of raw mineral resources required can be determined.
2. GHG fluxes, most commonly CO₂, into or out of mineral resources can be determined based on the stoichiometry of the reaction and are referred to as chemically derived emissions. For example, in the reaction to form lime from limestone (CaCO₃ → CaO + CO₂), one mol of CO₂ is released per mol of lime formed or 0.79 kg CO₂ / kg lime.
3. The thermodynamic energy requirement of the reaction can be determined based on the standard enthalpy of the reaction, calculated as the sum of the standard enthalpy of formation of the products minus the sum of the standard enthalpy of formation of the reactants, with the equation:

$$\Delta H_{Rxn,x} = \frac{\sum_{products} n_p \cdot \Delta H_{f,p}^o - \sum_{reactants} n_r \cdot \Delta H_{f,r}^o}{n_x} \quad (1)$$

In this equation, $\Delta H_{Rxn,x}$ is the enthalpy of reaction per mol of product, x , $\Delta H_{f,p}^o$ is the standard enthalpy of formation of each product, and n_p is the number of mols of each product, and similarly for each reactant, r .

We note that values of chemical CO₂ emissions and enthalpy of reaction for mineral-derived materials using production methods typically used in the United States have previously been tabulated.²² These tabulated values may provide additional guidance on determining these critical inputs for novel materials.

Separation, benefaction, and purification processes are often performed after mineral extraction, in biorefineries to separate biogenic constituents, or in the processing of fossil resources to eliminate impurities and separate co-products. Typically, these processes do not convert the chemical structure of the material extracted material but may lead to chemical reactions of other mineral material phases present, other reactants, or the formation of intermediate products. Therefore, a similar first-principles method can be applied to estimate LCI data as was done for chemical conversion. We note that GHG emissions associated with secondary inputs required for chemical reactions can be estimated via first principles using methods from chemical conversion, or a past LCI or proxy can be utilized. In industrial production, separation processes are often highly synergistic, yielding multiple products. Allocation of emissions to co-products can be performed or avoided using methods similar to those employed in conventional LCA.

For many biogenic materials, drying of moisture content is a key process step prior to other processing. For example, green logs may enter a mill at 50% moisture content and be dried to 10%. The enthalpy of vaporization for water dictates minimum drying energy (40.7 kJ/mol or around 2.3 MJ/kg of water).

To model mechanical processing, such as crushing, grinding, and milling processes, we implement Bond's equation²³, which relates the energy used during a size-reduction process (W) to the starting particle size

1 (80% passing particle size, F), ending particle size (80% passing particle size, P), and the Bond index, an
2 experimentally-derived constant specific to a particular mineral (W_i):

$$W = \frac{10 \cdot W_i}{\sqrt{P}} - \frac{10 \cdot W_i}{\sqrt{F}} \quad (2)$$

3
4
5 The Bond index has been reported for a wide variety of minerals by Bond²³ and has since been further
6 refined by additional studies. Energy use during mechanical processing was calculated with this
7 equation with P and F values typical for the input minerals post-mining and final material product.
8 Methods such as this, which directly relate energy inputs to the processing conditions of the resources
9 and products, can be utilized to inform LCIs for other grinding processes. For other mechanical
10 processing, such as sawmilling of wood, a ground-up approach is taken, utilizing data for mechanical
11 processing assembled from wood processing facilities such as sawmills and CLT mills. Based on the
12 type of product(s) and wood type (hardwood vs. softwood), a ground-up decision tree approach was
13 developed for sawmilling (Figure 9).

14 2.1.4 Manufacturing and material assembly

15 The first principles-based approach will inform direct enthalpy requirements for chemical conversion.
16 However, the inherent inefficiency of equipment must also be addressed to determine energy demand
17 and associated GHG emissions from energy resource use. Enthalpy requirements apply only to materials
18 that undergo chemical conversion, but energy inefficiencies apply broadly to material production. For
19 processes that use standard conversion technologies (e.g., blast furnaces, rotary kilns, final lumber
20 processing), process energy efficiency can be estimated using the efficiency of similar facilities,
21 considering both methods of conversion, process length, and process temperature. Data are widely
22 available for standard processes via numerous sources, such as the *Manufacturing and Energy*
23 *Conversion Survey (MECS)*, which is used herein.^{24,25}

24
25 For biomass drying, past estimates for total energy use range from 2.8 to 6 MJ/kg water, indicating that
26 the enthalpy of vaporization (2.3 MJ/kg water) provides a useful minimum, and drying efficiency may
27 vary from approximately 40-80% depending on technology.²⁶ Drying processes often combust residues
28 (biomass) to provide this energy but in some cases, another energy source is imported.

29
30 The energy grid and fuel mixtures used to generate energy for all material production and conversion
31 processes and their associated emission factors used to meet this energy demand can be estimated via
32 methods similar to conventional LCA, such as by using emission factors reported by the US
33 Environmental Protection Agency.²⁷ These emission factors can be applied to energy requirements
34 determined in earlier steps based on energy type (e.g., electric or thermal) and can then be modified to
35 examine the sensitivity of results to specific energy resources; see Supplemental Table 5 for the
36 emission factors used herein.

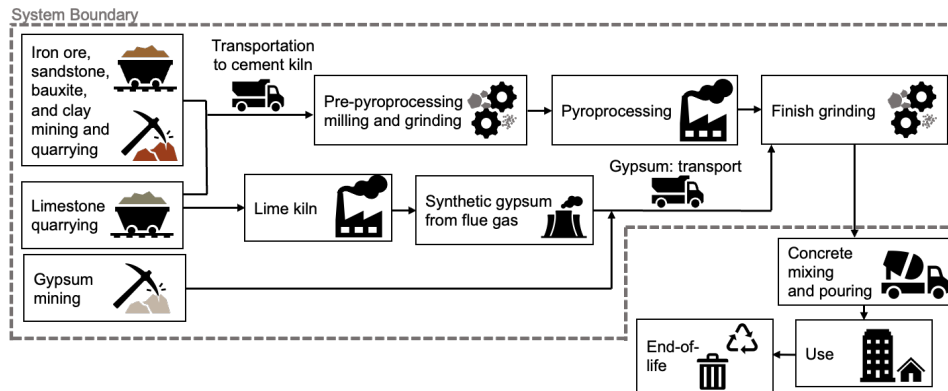
37
38 Beyond energy efficiency, material losses due to dust and spillage for mineral materials, as well as yield
39 efficiencies for biogenic materials, should be considered for all steps of the production process. We note
40 that material losses during chemical processing do not include chemically derived emissions, such as
41 CO₂ released from chemical reactions, which are accounted for separately. The impact of material losses
42 on total GHG emissions and energy requirements varies depending on the point of the losses during the
43 production process, so losses should be accounted for individually at each processing stage. If multiple
44 materials are combined into a full product (e.g., mixing of clinker and gypsum to form Portland cement
45 or resin and wood in CLT), material input LCIs should be combined at this step.

46
47 Transportation should be modeled as in conventional LCAs, based on established truck, rail, and boat
48 emission factors in kg CO₂e/kg·km.^{21,28} We note that transportation distances are highly site-specific and

1 may not be accurately estimated from lab or pilot-scale data. As with process efficiency, facility
 2 overhead, including facility HVAC, lighting, onsite transportation, and other facility energy
 3 consumption not associated with the direct production of materials, can draw data from existing analyses
 4 of comparable facilities (e.g., *MECS* for US-wide overhead values for common materials²⁴).

7 2.2 Framework validation for mineral-derived materials

8 To validate the developed framework, it is applied to several common mineral-based building materials,
 9 namely Portland cement, low-carbon steel, and gypsum board. For presentation purposes, we focus our
 10 discussion on Portland cement, which has global use, a variety of resource inputs, and broad availability
 11 of existing LCI data for comparison. Portland cement is examined with production processes and
 12 mineral feedstocks that are typical of primary production in the United States, with a cradle-to-gate
 13 scope and a functional unit of 1 kg of final material (Figure 2). For all data inputs, data from 2019 or the
 14 closest available year prior to 2020 is used. To validate the framework, we model the LCI of Portland
 15 cement as if quality LCI data does not exist. However, to obtain equivalent data that would be available
 16 for novel processes, we draw on existing process data that is representative of US average production.
 17 The details of the analysis for low-carbon steel and gypsum board are presented in the Supplemental
 18 Information, but we demonstrate the application of the framework to more complex thermal processing
 19 during steel production and composite materials and drying during gypsum board production.



21 **Figure 2.** Process flow diagram displaying the system boundary used for the LCI of Portland cement described herein.

22
 23
 24 Portland cement typically contains the mineral phases alite (Ca_3SiO_5), belite (Ca_2SiO_4), ferrite
 25 ($\text{Ca}_4\text{Al}_2\text{Fe}_2\text{O}_{10}$), and aluminate ($\text{Ca}_3\text{Al}_2\text{O}_6$), with gypsum ($\text{Ca}_2\text{SO}_4 \cdot 2\text{H}_2\text{O}$) added during finish grinding
 26 to control setting rate. The ratio of these mineral phases may vary depending on the type of Portland
 27 cement and processing facility but herein is modeled with ratios typical of Type I Portland cement (63%
 28 alite, 15% belite, 9% ferrite, 8% aluminate, 5% gypsum¹³) which comprises ~75% of US cement
 29 production.²⁹

30
 31 Mineral phase inputs are determined from chemical reactions of cement formation (Supplemental Table
 32 3), and the mineral inputs for these phases are from the USGS Mineral Yearbook (2019)²⁹ data and
 33 analyses of this data³⁰ for cement, excluding waste or byproduct resource inputs. Material losses due to
 34 dust, spillage, and other sources were considered, but literature values for material losses during these
 35 steps vary greatly by study.^{31–33} Further, the impact of this variation on total GHG emissions and energy
 36 requirements varies depending on the point of the losses during the production process, with fewer
 37 emissions embodied in losses prior to pyroprocessing. The NSF International Product Category Rule
 38 (PCR) for cement specifies a 5% estimate for material loss during production if other data is
 39 unavailable.³⁴ Past LCA studies report varying total material losses across the entire cradle-to-gate

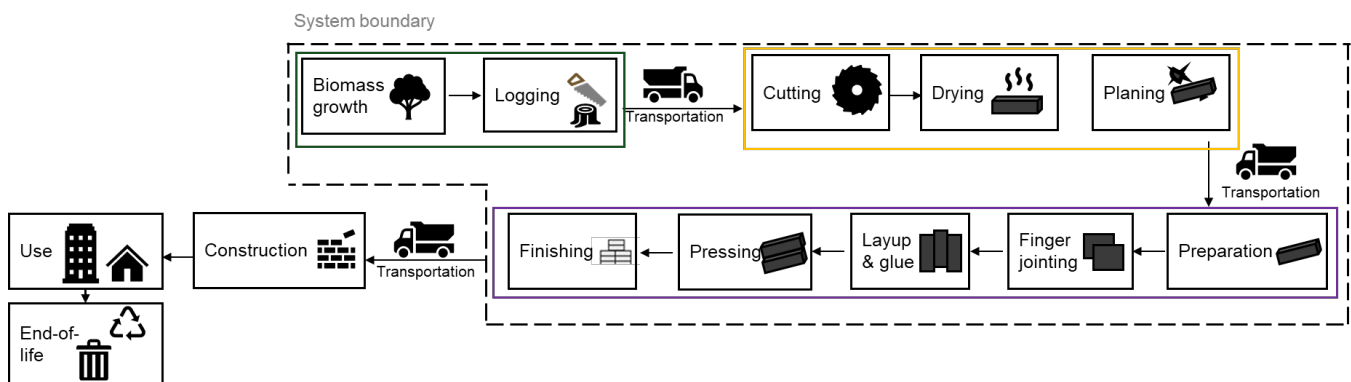
1 production process, typically 7-11 wt.%.^{31-33,35} Due to the meaningful variations in data for individual
 2 steps and to match these reported values for total material losses, values of 3% loss were used for all
 3 steps after mining, except storage, which was modeled as 1%, resulting in 10.4% total material loss
 4 across all process steps.

5
 6 Cement pyroprocessing is modeled as a single step, including preheating, pre-calcining, and the rotary
 7 kiln. Enthalpy of formation, resource requirements, and chemically-derived emissions from
 8 pyroprocessing are assessed from formation reactions for each mineral phase individually and then
 9 combined (Supplemental Table 3). No separation processes were modeled for Portland cement as these
 10 processes are not typically used in cement production. The mineralogy of raw mineral resources is
 11 determined from the literature.³⁶⁻⁴¹ However, we note that for some mineral resources, this is an area of
 12 significant spatial variation. LCIs for the mining and quarrying process of these materials are determined
 13 from ecoinvent,²⁰ using US data. Crushing and milling processes were modeled with Bond index values
 14 and particle sizes shown in the Supplemental Information, with electricity used as the energy source. An
 15 energy efficiency value of 54.5% was used, as determined from *MECS*, by dividing required energy by
 16 total energy inputs.²⁴ An average US electricity grid²⁷ and the average US fuel mix for cement
 17 production were used as electricity and fuel emission factors.⁴²

18
 19 Transportation is excluded from our mineral material case studies, given its high variability.⁴³
 20 Transportation distances between the mine or quarry and cement production facility are often considered
 21 negligible,⁴² as facilities are located at limestone quarries, and relatively small amounts of other minerals
 22 are used. However, potential future implementation of transportation distances is included in the
 23 developed framework.

24 2.3 Framework validation for biogenic materials

25 For biogenic materials, undergoing limited chemical processing, a limited first-principles approach can
 26 be combined with a ground-up decision-tree approach to assemble likely supply chains and individual
 27 processes required, making the assembly of the LCI more tractable. We address these assessment
 28 challenges by applying the framework to a case study of cross-laminated timber (CLT) products from
 29 yellow poplar (YP) and eastern hemlock (EH). The scope for YP CLT is shown in Figure 3 and details
 30 for EH CLT are provided in the Supplemental Information.
 31



33 **Figure 3.** Process flow diagram displaying the system boundary used for the LCI of YP CLT described herein. The green,
 34 yellow, and purple rectangle shows the harvest, sawmilling, and CLT mill processes, respectively.

35
 36
 37 The validation study conducted herein on YP CLT is based in Tennessee (TN), USA, as YP is abundant
 38 in the area, and sawmills in Tennessee already possess the equipment and knowledge necessary to

1 process YP logs for CLT manufacturing. CLT-specific considerations for a cradle-to-gate LCI include
2 forestry operations through the manufacturing of the CLT, highlighted in Figure 3. To model inputs to
3 CLT production, we have used a physical units-based input-output life-cycle inventory model, Agile-
4 Cradle-to-Grave (Agile-C2G), which has been documented in previous literature.⁴⁶⁻⁵¹ In this study, a
5 functional unit of 1 m³ of CLT was used for ease of comparison with previously published literature on
6 LCA of CLT. Life cycle inventory inputs and emission factors for each input parameter are provided in
7 Supplemental Table 5 and 6, respectively, based on previously published literature and LCA
8 databases^{15,19-21,52-55} and communications with local sawmills and was adjusted where necessary to
9 represent YP production. The assessment includes product transportation by truck between harvest to
10 sawmill (50 km), and sawmill to final CLT production (61.2 km).

11
12 For the GHG fluxes associated with wood harvest and transport operations, ground-up approach based
13 on the cradle-to-gate inputs and outputs of previously published literature^{63,64} and LCI databases to
14 incorporate material inputs for the harvesting stage that is specific for growth. Based on previous
15 literature,⁵⁶ our study assumes harvesting operations included the application of herbicides each year of
16 the growing period, and the trees were harvested after 21 years. For logging operations, it was assumed
17 that a shelterwood cutting method would be implemented using a feller buncher-based harvesting
18 system, and energy for logging was modeled based on previous literature.⁵⁶⁻⁵⁸

19
20 Using biogenic material properties and the final properties of the product, mass flows through each
21 process step can be estimated. Kiln-dried and sawn lumber is the wood input for the final processed
22 biogenic material considered in this study (i.e. CLT). The output from the sawmill is finished logs. The
23 sawmill processing steps include all debarking, sawing, chipping, and grinding required to convert the
24 logs to rough, dry lumber. The wood waste generated during the process is used in generating energy
25 onsite, with upstream emissions allocated on a mass basis. For this analysis, we considered fossil CO₂,
26 CH₄ and N₂O emissions and excluded biogenic CO₂ emissions. As with other processes, the sawmill
27 operational energy demand cannot readily be directly linked to the biogenic resource characteristics, so
28 data related to processes involved in the sawmill were adapted from the Southeast regions' data from
29 Milota and Puettmann.⁶⁵ The weighted average amount of wood in a CLT panel is 427 kg/m³. To
30 produce this amount, a total of 517 kg (1.21 m³) of oven-dry lumber is required.^{15,59} This dry wood
31 would, in turn, need 869 kg of green wood. Of this, 83% is assumed to be utilized to produce CLT,
32 while the rest is assumed to be co-product (sawdust, chips, shavings, etc.).^{15,59}

33 **3. Results**

34 A decision tree for the developed framework is shown in Figure 4, with details of the developed ground-
35 up analysis for forestry and logging provided in Figure 9. Validation examples of the application of this
36 framework are given below for key materials.

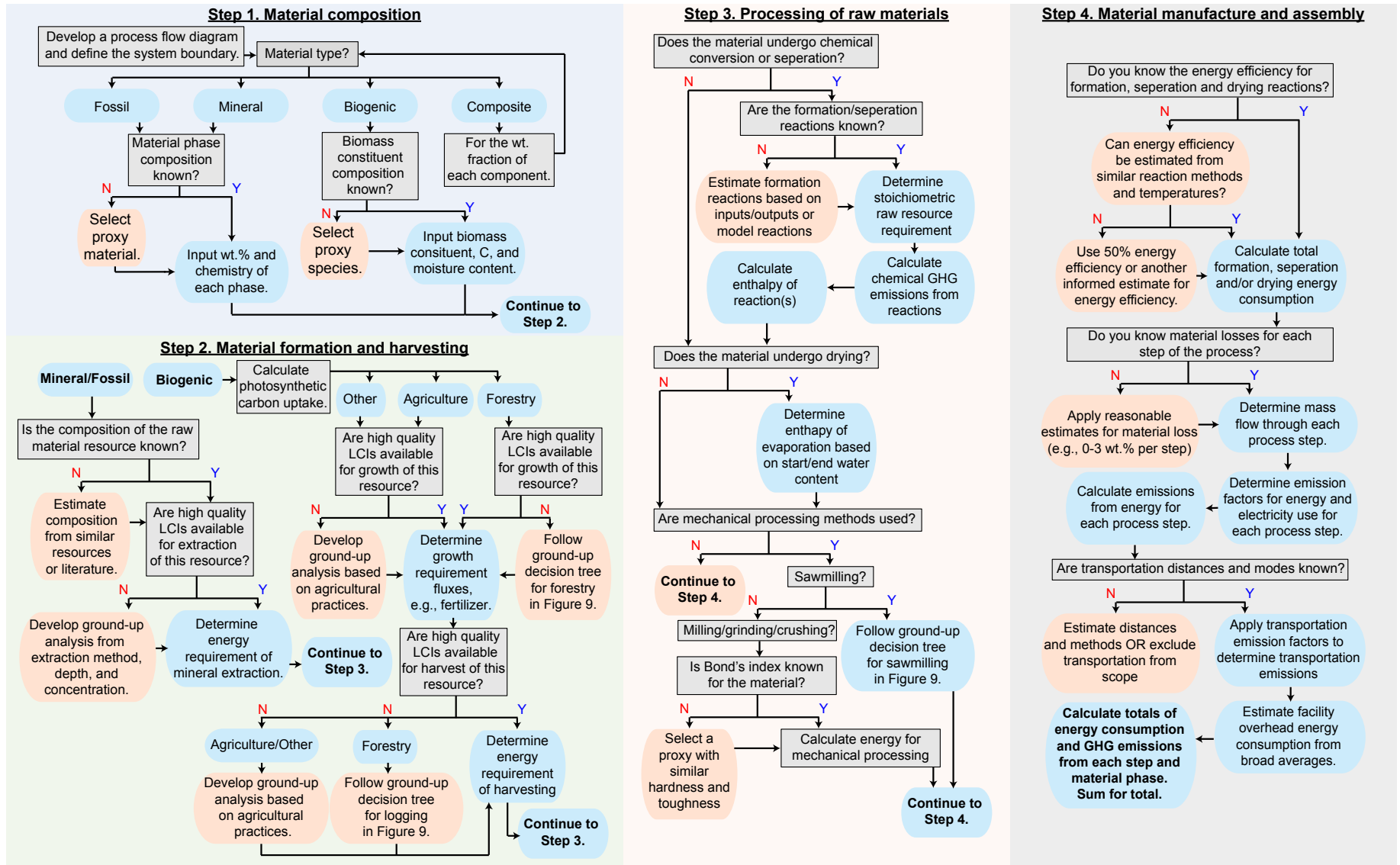


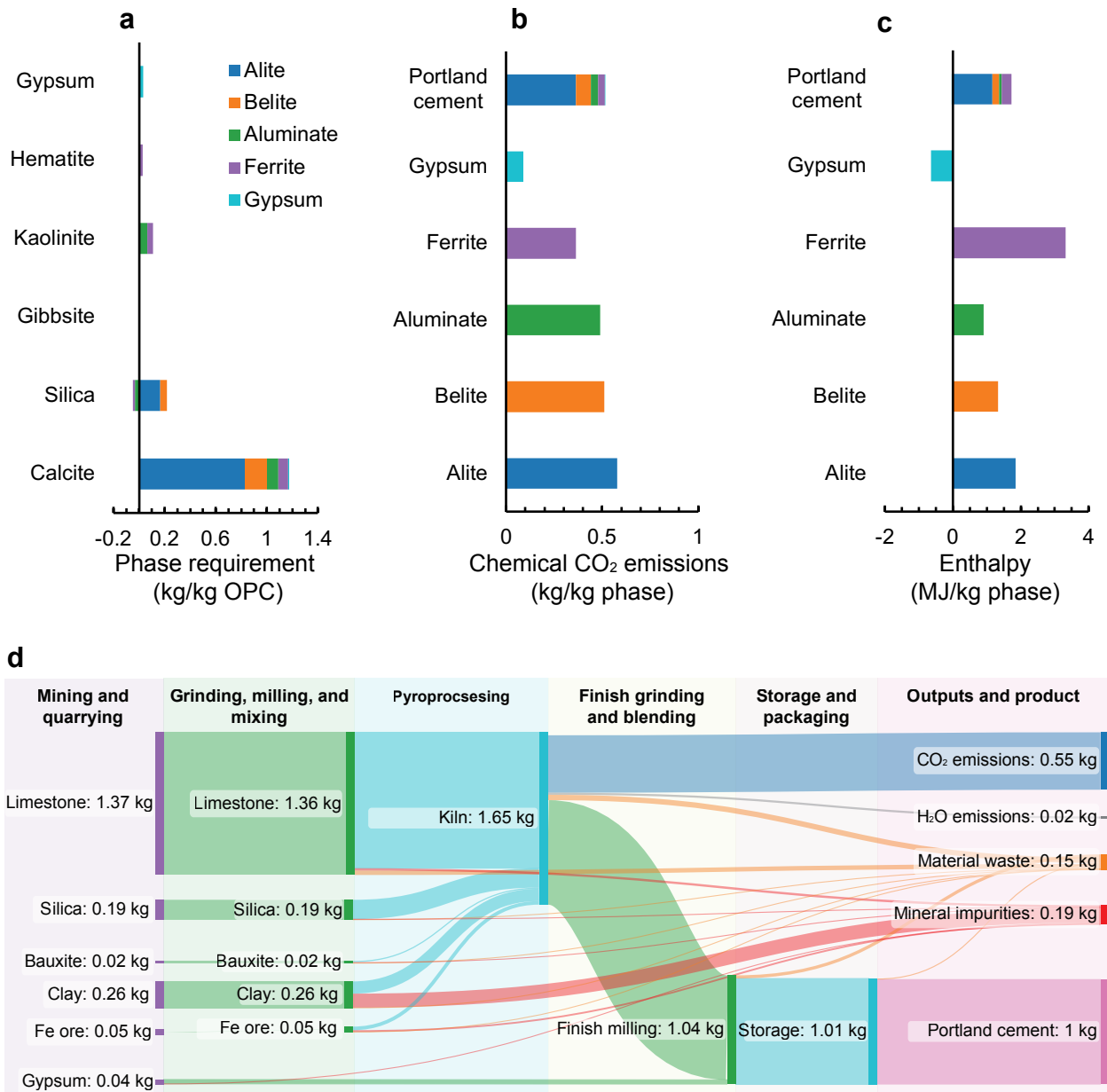
Figure 4. Decision tree of the developed ground-up framework for determining an LCI of a material.

1
2
3
4
5
6
7
8
9

3.1 Complete assessment and validation of Portland cement

3.1.2 Material formation and harvesting

From the formation reactions of Portland cement, mineral phase requirements were stoichiometrically determined and are shown in Figure 5a. As a result of impurities, mass loss due to material waste, and chemically-derived emissions, a total mass of 1.97 kg mineral is extracted / kg Portland cement, with the distribution of minerals shown in Figure 5d. Extraction of these resources requires 0.165 MJ / kg Portland cement energy consumption.



10
11
12
13
14
15
16

Figure 5. The first principle values for the chemical conversion of raw resources into cement include (a) mineral phase requirement, (b) chemically derived CO₂ emissions, and (c) energy required by the enthalpy of the reaction. Results in (b) and (c) are displayed for 1 kg of each cement phase and the total of 1 kg of Portland cement. (d) Sankey diagram of mass flows through the Portland cement production process showing raw resource requirements, material losses, material purity, and chemical emission values used in the first principle LCI. We note that in some cases, material impurities may instead be double-counting of consumed material that was not considered herein (e.g., silica in clay).

1
2
3
4 *3.1.3 Processing of raw materials*

5 Chemically-derived CO₂ emissions resulting from different Portland cement production pathways are
6 weighted based on the mass ratios of each method (Supplemental Table 3, Figure 5b), resulting in
7 chemically derived emissions of 0.548 kg CO₂ / kg Portland cement. The enthalpy of reaction for the
8 production of Portland cement is 1.70 MJ / kg Portland cement, with a majority of the contribution being
9 due to the alite phase (1.16 MJ / kg Portland cement, Figure 5c). Production reactions for aluminate
10 from bauxite and synthetic gypsum from calcite are exothermic. For the production of aluminate from
11 bauxite, this reaction would occur simultaneously with other endothermic reactions during cement
12 making and, therefore, is credited against their energy requirements. In contrast, synthetic gypsum
13 production is performed as an independent process, and its energy is not typically recaptured, so
14 therefore, it is not included in the energy total.

15
16 Grinding and milling processes prior to pyroprocessing result in an energy consumption of 0.215 MJ /
17 kg Portland cement, primarily due to limestone (0.153 MJ / kg), while post-pyroprocessing milling and
18 grinding results in an energy consumption of 0.118 MJ / kg.

19
20 *3.1.4 Material manufacture and assembly*

21 The modeled pyroprocessing efficiency of 54.5% results in a 1.76 MJ / kg Portland cement increase in
22 the energy consumption over the enthalpy. Further, with the modeled rates of material waste, 0.146 kg
23 of additional material is processed through at least one step, with an increase in mass flow through the
24 high emission and energy requirement pyroprocessing step of 7.15%. Facility overhead values, inclusive
25 of HVAC, onsite transportation, and facility lighting result in energy consumption of 0.04 MJ / kg
26 Portland cement. We note that due to the limited number of significant figures present in the *MECS* data,
27 this is an area of significant uncertainty and likely an area where there are large variations between
28 cement production facilities. However, given the small contribution of this value to net emissions, we
29 expect this to have a limited impact on the final results.

30
31 *3.1.5 Portland cement total energy and GHG emissions validation*

32 In total, the energy consumption of Portland cement production is dominated by the pyroprocessing
33 process, with 85% of the total energy consumption resulting from pyroprocessing and 42% of the total
34 energy consumption required by pyroprocessing enthalpy of reaction (Figure 6). Similarly, GHG
35 emissions from the production of Portland cement are dominated by pyroprocessing, with 59% of total
36 GHG emissions resulting from chemically derived emissions during pyroprocessing.

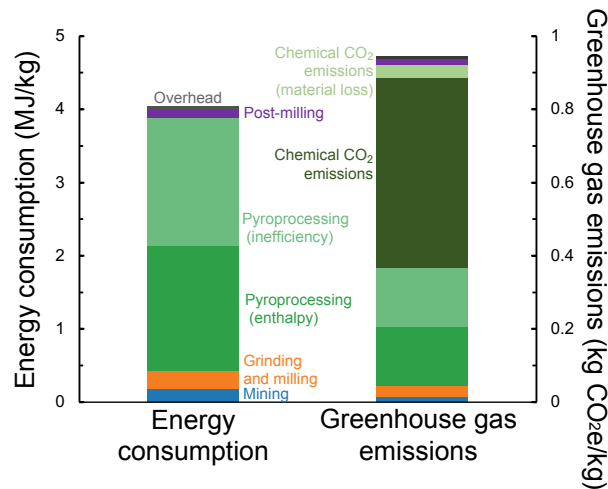


Figure 6. Totaled results for energy and GHG emissions for Portland cement, showing the contribution of each process step.

The GHG emissions determined with the ground-up approach (0.94 kg/kg Portland cement) are in good agreement with the value determined by the PCA EPD (0.92 kg/kg Portland cement).⁶⁰ Similarly good agreement is seen in the chemical emissions resulting from pyroprocessing (this study: 0.548 kg CO₂-eq / kg, PCA: 0.480 kg CO₂-eq / kg Portland Cement) and energy consumption (this study: 4.04 MJ / kg, PCA: 3.88 MJ / kg). The small differences between these analyses is driven by a difference in clinker content of 95% in our model versus 91.4% in the PCA EPD. When normalizing by clinker content, both the ground-up LCI and the PCA EPD show energy consumption of 4.25 MJ / kg clinker.

The GHG emissions determined herein also agree with other broad analyses of the cement industry. For example, the Cement Sustainability Initiative, in an analysis of 618 cement production facilities globally, reports average GHG emissions of 0.842±0.101 kg CO₂e / kg Portland cement⁶¹. These emissions are again comparable to the values determined herein (within one standard deviation for GHG emissions and within 3% for energy consumption). As global production is expected to have lower clinker content than US production, the lower emissions are again primarily due to this factor. Similarly, the US LCI entry for Portland cement ("Portland cement, at plant, US"²¹) reports GHG emissions of 0.927 kg CO₂e / kg Portland cement, 1.7% lower than the value determined herein, and energy consumption of 5.47 MJ / kg Portland cement.

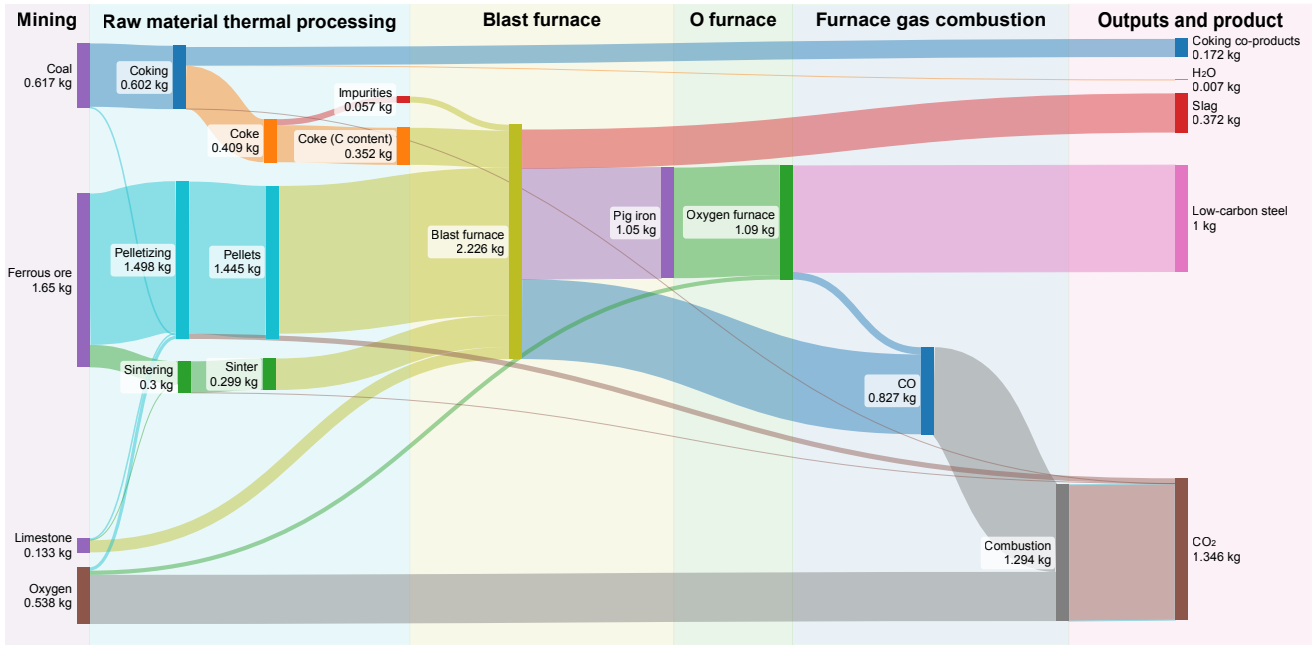
3.2 Challenges presented by other common mineral-derived materials

In addition to Portland cement, the developed framework was validated for low-carbon steel and regular-type gypsum board (See Supplemental Information for full methods and results). A mass flow diagram of steelmaking and gypsum board production is shown in Figure 7, and process flow diagrams are shown in Supplemental Figures 1 and 2.

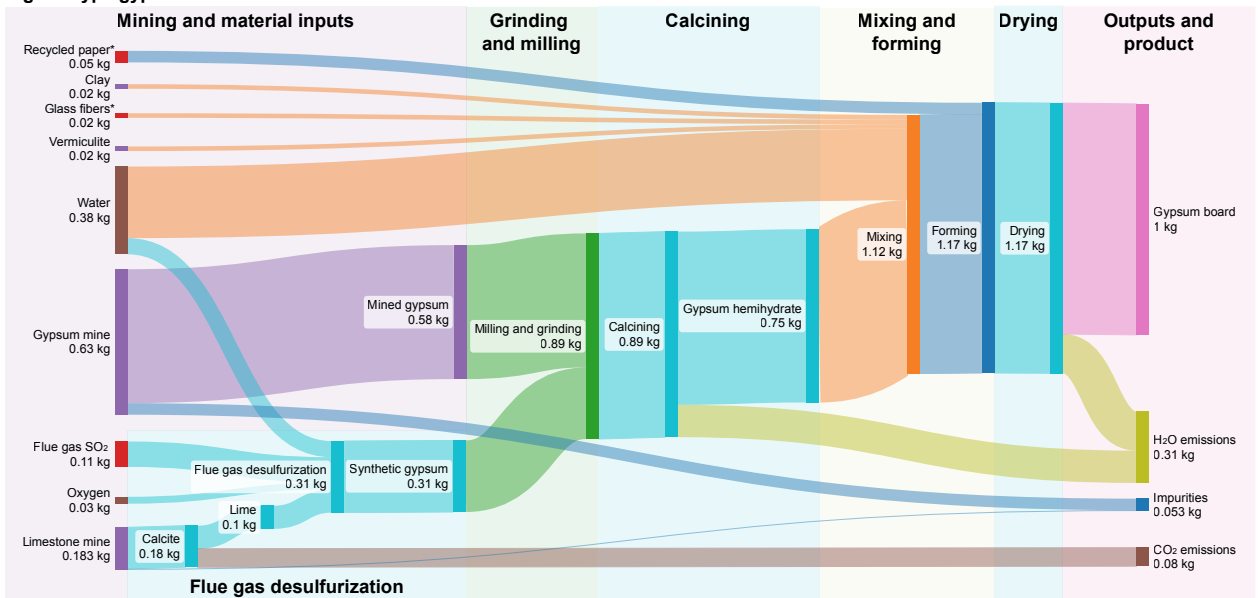
Steelmaking results in slag, coking gas, and blast furnace gas co-products. In the primary analysis, no emissions are allocated to the slag co-product. In comparison with Worldsteel⁶² and International Energy Agency (IEA)⁶³ steel emission values, we apply a system expansion approach to account for slag replacement of primary cement production, using the emissions and energy for cement production from the analysis performed herein. No allocation is performed to coking co-products – all emissions associated with potential downstream processing or use of these products are excluded. We examine three allocation scenarios for CO₂ emissions associated with the oxidation of carbon monoxide produced by the reduction of iron ore to the energy co-product: (1) all oxidation emissions allocated to low-carbon

1 steel, (2) system expansion to include equivalent primary electricity production, and (3) all oxidation
 2 emissions allocated to electricity.

a Low-carbon steel



b Regular-type gypsum board

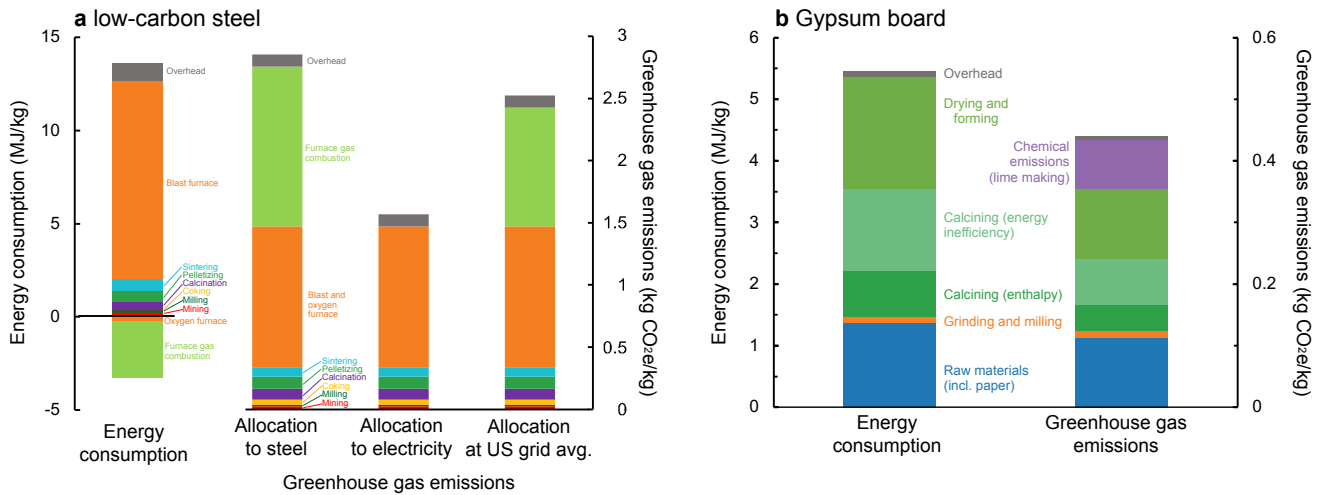


3 **Figure 7.** Sankey diagram of mass flows in (a) steel making and (b) gypsum board production. Material losses are excluded
 4 for clarity. Note that masses of coal for coking only include stoichiometrically required coke. Inputs for energy use are not
 5 shown.
 6
 7

8 The chemically derived CO₂ emissions of steelmaking are dominated by the combustion of blast furnace
 9 (1.12 kg CO₂/kg steel) and oxygen furnace (0.11 kg CO₂/kg steel) gas to CO₂ (Supplemental Figure 3a).
 10 In the scenario where these emissions are allocated to steel, these emissions comprise 93% of all
 11 chemically derived emissions, with total chemical-derived emissions of 1.32 kg CO₂/kg steel. Therefore,
 12 in the scenario where all these emissions are allocated to the energy product, chemically derived
 13 emissions are greatly reduced to 0.09 kg CO₂/kg steel, driven by the calcination of limestone to form

1 lime (0.06 kg CO₂/kg steel), and coking (0.03 kg CO₂/kg steel). The system expansion allocation
2 scenario for these emissions results in chemical-derived CO₂ emissions of 1.02 kg CO₂/kg steel.

3
4 When all emissions are allocated to steel, steelmaking emits 2.854 kg CO_{2e} / kg steel, driven largely by
5 chemical emissions from the combustion of blast furnace and oxygen furnace gases (89). Energy
6 emissions due to blast furnace enthalpy and inefficiency in energy consumption make up the majority of
7 remaining emissions, and combined, these three categories comprise 85% of total GHG emissions.
8



9
10 **Figure 8.** Energy consumption and total GHG emissions from (a) steelmaking for the three allocation scenarios considered
11 and (b) gypsum board production.

12
13 In total, 13.7 MJ of energy is consumed to produce 1 kg of steel, and 3.3 MJ of energy is produced.
14 Energy consumption is dominated by blast furnace enthalpy and inefficiency, which consume 78% of
15 the total energy consumption. Produced energy is primarily due to furnace gas combustion, with only
16 0.27 MJ/kg steel energy being produced in the oxygen furnace, which is modeled as not recovered in all
17 allocation scenarios.

18
19 To validate the developed framework, the herein developed model is compared against LCAs of steel by
20 the IEA⁶³ and Worldsteel.⁶² We make our comparison with the system expansion energy allocation for
21 furnace gas combustion and, additionally, to match the assumptions made by these past analyses, apply
22 system expansion to the slag co-product, considering the replacement of primary cement clinker at the
23 GHG emissions and energy consumption determined with the ground-up model for cement. As a result
24 of the production of 0.3 kg of slag, the GHG emissions of this scenario are reduced by 0.27 kg CO_{2e} / kg
25 of steel, resulting in emissions of 2.25 kg CO_{2e} / kg steel. This result is comparable to emission values
26 from both the IEA and Worldsteel of 2.2 kg CO_{2e} / kg steel. Total energy consumption in this scenario
27 is modeled as 12.51 MJ / kg steel.

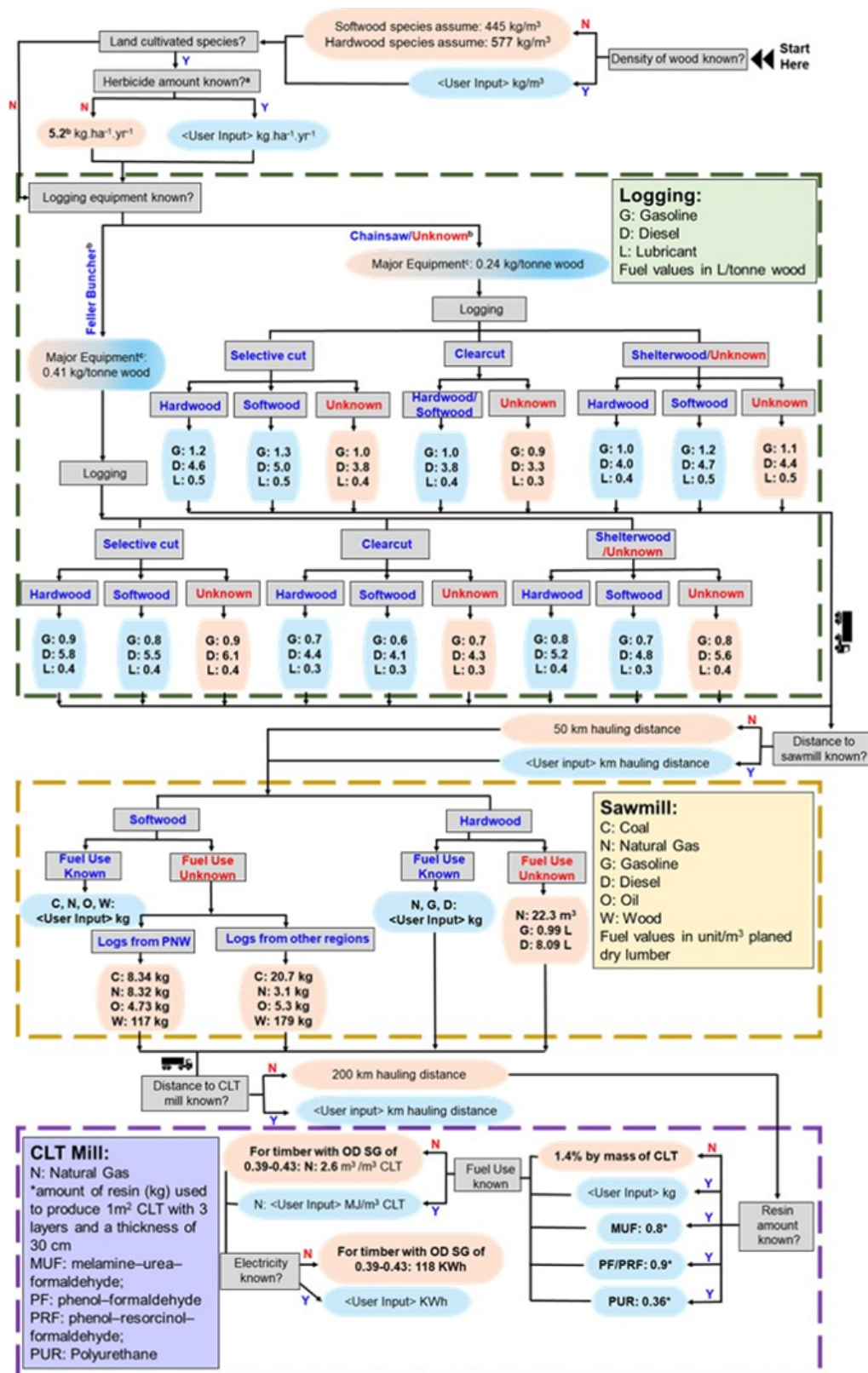
28
29 Gypsum board is a material used on walls that is primarily composed of a gypsum core (typically with
30 glass fiber reinforcement) sandwiched between sheets of paper. Unlike Portland cement and low-carbon
31 steel, where chemical conversion is the primary driver of emissions, the energy consumption of gypsum
32 board production is dominated by drying processes (Supplemental Figure 4c), which consume 33% of
33 the total energy (Figure 8b). The water content, and therefore drying energy requirement, of gypsum
34 board can be highly variable depending on production facility practices and can result in large variations
35 in LCA data. Material inputs of recycled paper play the next largest role in energy consumption, at 60%
36 of raw material extraction energy consumption and 15% of total energy consumption, respectively. In

1 this work, we considered the glass and paper as already processed to demonstrate the integration of
2 existing LCI data for known products with the developed framework to assess composite materials. Due
3 to the production of synthetic gypsum, 19% of total GHG emissions result from chemically derived
4 emissions— primarily the calcination of limestone to lime prior to sulphuration, noting that no allocation
5 is assigned to the capture of SO₂.

6 The total energy consumed to produce 1 kg gypsum board was modeled as 5.46 MJ, which is in the
7 range of previously reported energy use of 3.44-6.74 MJ/kg gypsum board.⁶⁴⁻⁶⁹ In addition, the variation
8 in kiln efficiency, paper recycling technologies, and the amount of excess water that needs to be
9 evaporated (e.g., if more water than required is added to aid in forming) could also cause variations in
10 energy requirement. To accurately consider scenarios such as gypsum board, where evaporation (or
11 other phase change reactions) plays a critical role in net emissions, careful consideration of potential
12 recapture (e.g., during condensation) or use (e.g., as steam) should be considered.

14 **3.3 Complete assessment and validation of yellow poplar CLT**

15 To validate an application to a biogenic material, we applied the framework to cross-laminated timber
16 (CLT) produced from YP. Typically, CLT is produced from softwoods based on composition and
17 flexibility advantages and has a greater wealth of LCI data.^{15,70} YP is an emerging alternative for CLT to
18 allow for greater diversity in materials and local sourcing and allows for the framework to be applied to
19 a more data-scarce product, highlighting the flexibility of the framework. In our SI, we have also
20 provided the framework application to CLT from EH for further validation of the framework. Figure 9
21 shows the decision tree for the ground-up analysis performed in the framework given in Figure 4 applied
22 to logging and forestry practices.



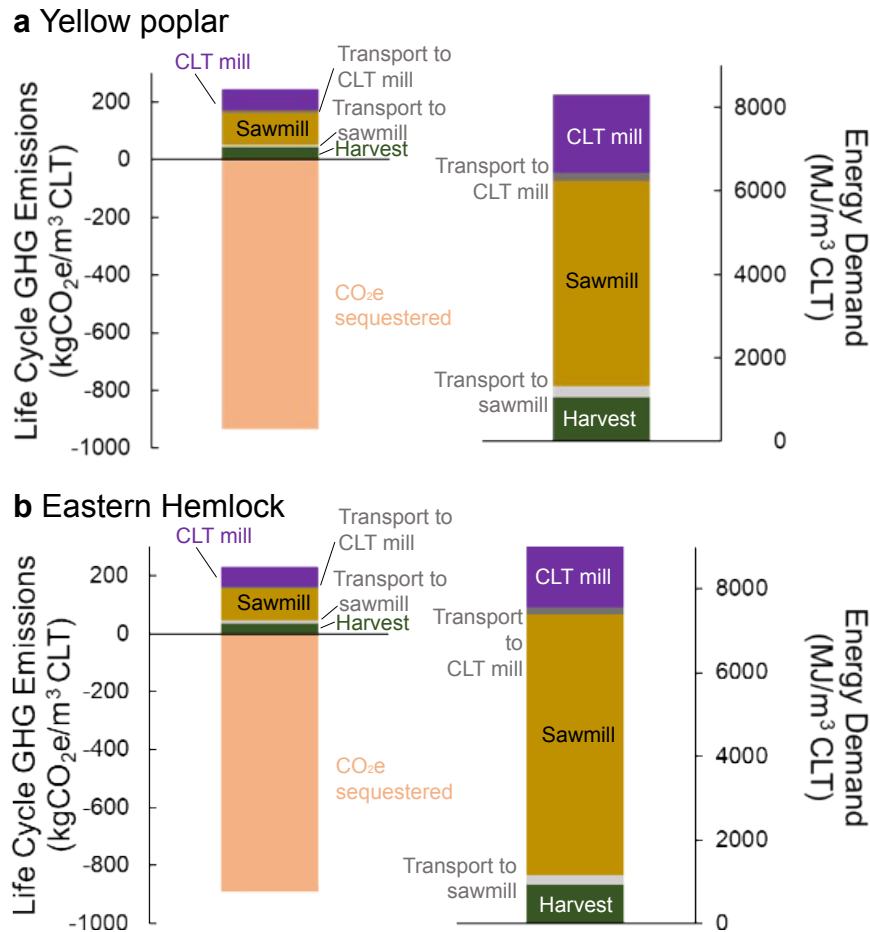
*Herbicide is assumed to be comprised of 25% atrazine, 25% metolachlor, 25% acetochlor and 25% cyanazine by mass (kg).
 †If the sawmill is a medium-sized one, assume use of feller buncher-based harvesting system for logging operations. If sawmill size is unknown, or logging equipment information unknown, assume use of chainsaw-based harvesting system.
 ‡Major harvesting equipment considerations include both use and maintenance of the harvesting equipment when calculating impact on GHG emissions.

Figure 9. Decision tree of the developed framework for a biogenic material grown with forestry practices.

1
2
3

1 *3.1.5 Yellow poplar CLT total energy and GHG emissions validation*

2 Here, we present results focusing on the GHG emissions for CLT. GHG fluxes are primarily tied to the
 3 energy demand and resources used. As such, we present GHG emissions and energy demand for the
 4 cradle-to-gate production of 1 m³ of CLT (Figure 10). The majority of the GHG emissions are
 5 associated with the lumber production in the sawmill (~ 46% of total kg CO₂e emissions per m³ CLT),
 6 followed by the emissions associated with CLT production (~ 28% of total kg CO₂e emissions per m³
 7 CLT). Transportation-related emissions are dependent on the routes taken by the truck and the load
 8 carrier, and as such, these emissions for the present study are minimal for the haul to the sawmill (9.5 kg
 9 CO₂e/m³ CLT) and CLT mill (6.9 kg CO₂e/m³ CLT). The energy demand results show that almost 63%
 10 of the total energy consumption occurs during the operations in the sawmill to produce lumber that
 11 serves as feedstock for the CLT mill. However, a portion of this demand is met by the renewable
 12 biomass (shavings, chips, etc.) generated onsite.



13 **Figure 10:** Life Cycle Greenhouse Gas Emissions and Energy Demand for the cradle-to-gate production of 1 m³ CLT using
 14 (a) YP and (b) EH as a source of wood.
 15
 16
 17

18 *3.1.6 Accounting for biogenic carbon*

19 1 m³ of CLT stores 933 kg CO₂e based on a carbon content of 50% of the wood. From this, the net
 20 cradle-to-gate GHG emissions are approximately -691 kg CO₂e / 1 m³ of CLT.
 21

22 The GHG emissions modeled herein for CLT are consistent with previously published results^{15,53,55}, with
 23 slight variations due to the difference in the source of the lumber. GHG emissions are primarily a
 24 function of energy demand, and our energy demand results for the sawmill operations stage (4932 MJ

1 /m³) are higher than results published in some sources^{15,55}, but are in agreement with the previously
2 published energy demand data for Southeast (SE) region lumber production (reported as 5151 MJ/m³
3 dry lumber)⁵⁶; our results are within 4% of this value. This variation may be due to the approximations
4 used in this study being based on the North American Electric Reliability Corporation's SERC region
5 electricity grid mix and YP as the source of lumber. In this study, the SERC grid mix was utilized for
6 electricity demand calculations, as the facilities are assumed to be based in TN. However, the US
7 electric grid mix is well characterized for all states, and the US average grid mix could be used to
8 estimate emissions for a generalized case study. Additionally, the use of facility-specific equipment and
9 processes (such as the use of chainsaws and a clear-cut method for logging operations rather than feller
10 buncher-based felling operations and the shelterwood method of thinning assumed in this study) can be
11 integrated into this framework if material producers seek more specific results.

13 **3.4 Challenges presented by other biogenic materials**

14 Due to the wide variety of potential biogenic materials and product types, LCA researchers should
15 closely consider the variations we have outlined in the framework and highlighted in the case study of
16 YP CLT. As shown in Figure 10 of the case study results, carbon sequestered via photosynthetic growth
17 can substantially impact the results and can have the greatest amount of variability. When assessing a
18 biogenic product, researchers should consider using a range of sequestration values, such as those
19 tabulated in Supplemental Table 2.

21 Processing and manufacturing represent the second-largest contributions to life-cycle impacts. Obtaining
22 primary data (e.g., fuel use, equipment, yield, and energy efficiencies) from processing and
23 manufacturing facilities offers the greatest accuracy in developing an LCI, but existing literature or
24 proxy materials can be a substitute. Identifying the potential greatest sources of life-cycle impacts and
25 focusing efforts on reducing uncertainties for these stages, whether through accessing specific data or
26 modeling a range of inputs, can bolster the accuracy and effectiveness of future biogenic LCA material
27 research.

29 The developed framework focused on forestry, as forest products represent a majority of biogenic
30 material used industrially. However, a similar approach could be taken for agricultural crops by
31 considering appropriate energy inputs for cultivation and harvesting, as well as fertilizer, herbicide, and
32 other inputs to agriculture to develop a similar ground-up calculation to those developed herein for
33 forestry and logging. Similarly, an adapted approach could be taken for marine biomass (such as algae
34 or seaweed) growth for use in biofuel processes or materials. For non-photosynthetic biogenic processes
35 (e.g., fungi or microbial), a similar approach could be taken as mineral-derived processes.

37 Some biogenic materials may undergo chemical processing after production, for example, in the
38 production of paper, bioethanol, bio-based plastics, or bio-based carbon materials. These chemical
39 separation or conversion processes can be modeled similarly to those described for mineral-derived
40 materials, as shown in Figure 4.

41 **4. Discussion**

42 We have validated the developed framework against conventional Portland Cement, low-carbon steel,
43 gypsum board, and two types of CLT. However, the primary application is expected to be novel building
44 materials and identifying low or negative-carbon materials that may aid infrastructure in transitioning
45 from carbon-emitting to carbon-sequestering. The analysis of novel materials presents several additional
46 challenges with data availability; these can be addressed with the developed decision trees (Figures 2, 4
47 and 10), showing alternative paths that may be taken to generate an inventory of novel materials. For

1 materials that undergo chemical conversion, a critical area for consideration is process thermal
2 efficiency. This is the case for many mineral-derived materials but also could be applied to chemical
3 processing of biogenic materials, or refinement of fossil-derived materials. We expect this to play a
4 critical role in total energy consumption and GHG emissions, as seen in the data for Portland cement and
5 low-carbon steel. For biogenic materials, obtaining carbon storage region-specific data for a given
6 species or modeling a range of storage values across regions is important for understanding the greatest
7 uncertainties in biogenic material LCA modeling.

8
9 We expect that for most novel materials, the chemical composition and chemical synthesis processes
10 will be well defined by experimental data, allowing for raw resource requirements, enthalpy of
11 formation, and chemically derived emissions of the formation reaction to be determined. If composition
12 is not known, it can be estimated using representative compounds or averaging bulk properties (see, for
13 example, biochar production via pyrolysis ⁷¹). Novel compounds may utilize more poorly
14 thermodynamically characterized mineral resources or material phases, in which case, enthalpy of
15 formation values may need to be experimentally determined. In addition, the mineralogy of raw
16 resources may be more poorly characterized, or the mineral used as a feedstock may eventually differ
17 between laboratory and commercial scale, leading to differences in both formation and separation
18 reactions and resource extraction, which may necessitate consideration of diverse mineral resources in
19 initial assessments to accurately gauge the range of LCI values. While for conventional materials, LCIs
20 will typically be available for mineral resource extraction, for novel materials, this may not be the case,
21 and therefore, a ground-up approach should be taken to develop LCI that estimate energy consumption
22 based on mineral hardness, extraction depth, mining methods, etc., with a similar scope of analysis as is
23 taken for forestry and logging herein. Bond index values or particle sizes may not be available for novel
24 processes, in which case experimental data may be needed, or proxy materials based on hardness and
25 mineralogy should be used. Process energy efficiency, material efficiency, and facility overhead may be
26 highly uncertain for novel materials and may necessitate uncertainty assessment to determine
27 distributions of LCI outcomes (see previous analysis of biochar⁷² and cement⁷³ for examples of pairing a
28 ground-up LCA approach with uncertainty assessment). Additionally, the production of novel materials
29 may have processing steps not considered in the developed framework (e.g., forming processes). We
30 anticipate that the energy requirement for many of these processes can be modeled with first principles
31 or ground-up approaches in a similar method to those examined herein; for example, the energy
32 requirement of steel casting could be estimated based on the melt enthalpy of steel and heat transfer out
33 of the steel during processing. This work does not aim to provide exact guidance on each situation that
34 may occur in novel materials. Instead, it provides a generalized framework that may be interpreted to fit
35 unique, novel materials and processes to improve the accuracy of first-principle LCIs and lessen data
36 gaps between first-principle methods of estimating LCIs and computationally expensive process
37 simulations.

38
39 The primary role of the framework developed herein was to provide a step-by-step, repeatable process
40 for determining the life-cycle GHG emissions of novel materials and processes. Building on this
41 framework, similar methods could be applied to determine other lifecycle impacts. Knowledge of
42 material reactions can be applied to determine other outputs to the environment from chemical reactions
43 (e.g., SO₂ in roasting of metal sulfide ores) and similar combinations of existing LCIs for known
44 processes and modeling novel processes from first principles. Some emissions, such as particulate
45 emissions, may be particular to facility design or operation conditions. In these cases, standard proxy or
46 estimation methods should be used. These methods will provide similar data quality to existing methods,

1 while data quality for methods that can be accurately modeled with first-principle or ground-up LCI will
2 be improved by the developed framework.

3
4 For biogenic materials, novel materials present significant data challenges that can be overcome with the
5 developed ground-up approach, particularly in the stages that will contribute the most to life-cycle
6 impacts (i.e., carbon storage, processing, manufacturing). Our case study application of YP CLT reflects
7 an emerging feedstock for CLT production, where data challenges were significant in processing and
8 manufacturing. Working with the facilities directly to obtain primary data and validating this approach
9 with YP material experts allowed this framework to reduce uncertainties for this novel lumber material.
10 Since novel biogenic materials can come from a wide variety of feedstocks, future framework
11 applications should determine early in the assessment process where data gaps are most significant and
12 begin to contact experts and practitioners to obtain primary or (in the case of missing data) proxy data to
13 start mitigating uncertainties and data gaps early in the process.

14
15 As novel materials, systems, and products continue to be developed to decarbonize industrial sectors, the
16 framework presented herein can help to address critical data gaps in LCI data early in the research and
17 development process. By providing a systematic method to improve the accuracy of first-principle LCIs,
18 GHG emissions are critical data for industrial decarbonization that can be estimated for novel materials.
19 We believe this framework has broad applicability to the development of novel materials for broad
20 applications, including decarbonizing building materials, carbon sequestration in materials, biofuels, and
21 bioproducts, and the development of novel energy materials and technologies.

22 **Acknowledgements**

23
24 S.K., J.F., B.B., T.H., C.D.S., and S.M.'s contribution to this work was funded through the US
25 Department of Energy, Advanced Research Projects Agency-Energy (ARPA-E, Grant #DE-
26 AR0001625). This article represents the views of the authors, not necessarily those of the funder. This
27 work was supported in part by the U.S. Department of Energy, Office of Science, Office of Biological
28 and Environmental Research, through contract DE-AC02-05CH11231 between Lawrence Berkeley
29 National Laboratory and the U.S. Department of Energy. The U.S. Government retains and the
30 publisher, by accepting the article for publication, acknowledges that the U.S. Government retains a
31 nonexclusive, paid-up, irrevocable, worldwide license to publish or reproduce the published form of this
32 manuscript, or allow others to do so, for U.S. Government purposes.

33 **References**

- 34 1 S. Kane and S. A. Miller, Greenhouse gas emissions of global construction material production,
35 *Environmental Research: Infrastructure & Sustainability*.
- 36 2 E. G. Hertwich and R. Wood, The growing importance of scope 3 greenhouse gas emissions from
37 industry, *Environmental Research Letters*, 2018, **13**, 104013.
- 38 3 National Academies of Sciences, Engineering, and Medicine, *Gaseous Carbon Waste Streams*
39 *Utilization: Status and Research Needs*, National Academies Press, 2019.
- 40 4 E. Van Roijen, S. A. Miller and S. J. Davis, Building materials could store more than 16 billion
41 tonnes of CO₂ annually, *Science*, 2025, **387**, 176–182.
- 42 5 Organisation for Economic Co-operation and Development (OECD), *Global Material Resources*
43 *Outlook to 2060: Economic Drivers and Environmental Consequences*, 2019.
- 44 6 International Energy Agency, *Material efficiency in clean energy transitions*, 2019.
- 45 7 J. L. Rivera and J. W. Sutherland, A design of experiments (DOE) approach to data uncertainty in
46 LCA: application to nanotechnology evaluation, *Clean Techn Environ Policy*, 2015, **17**, 1585–1595.
- 47

- 1 8 F. Piccinno, R. Hischer, S. Seeger and C. Som, From laboratory to industrial scale: a scale-up
2 framework for chemical processes in life cycle assessment studies, *Journal of Cleaner Production*,
3 2016, **135**, 1085–1097.
- 4 9 S. Zargar, Y. Yao and Q. Tu, A review of inventory modeling methods for missing data in life cycle
5 assessment, *Journal of Industrial Ecology*, 2022, **26**, 1676–1689.
- 6 10 A. G. Parvatker and M. J. Eckelman, Comparative Evaluation of Chemical Life Cycle Inventory
7 Generation Methods and Implications for Life Cycle Assessment Results, *ACS Sustainable Chem.*
8 *Eng.*, 2019, **7**, 350–367.
- 9 11 N. von der Assen, J. Jung and A. Bardow, Life-cycle assessment of carbon dioxide capture and
10 utilization: avoiding the pitfalls, *Energy Environ. Sci.*, 2013, **6**, 2721–2734.
- 11 12 J. L. Hau, H. Yi and B. R. Bakshi, Enhancing Life-Cycle Inventories via Reconciliation with the
12 Laws of Thermodynamics, *Journal of Industrial Ecology*, 2007, **11**, 5–25.
- 13 13 S. A. Miller and R. J. Myers, Environmental Impacts of Alternative Cement Binders, *Environmental*
14 *Science and Technology*, 2020, **54**, 677–686.
- 15 14 K. Sahoo, R. Bergman and T. Runge, Life-cycle assessment of redwood lumber products in the US,
16 *Int J Life Cycle Assess*, 2021, **26**, 1702–1720.
- 17 15 C. X. Chen, F. Pierobon and I. Ganguly, Life Cycle Assessment (LCA) of Cross-Laminated Timber
18 (CLT) Produced in Western Washington: The Role of Logistics and Wood Species Mix,
19 *Sustainability*, 2019, **11**, 1278.
- 20 16 Y. Wang, R. Rasheed, F. Jiang, A. Rizwan, H. Javed, Y. Su and S. Riffat, Life cycle assessment of a
21 novel biomass-based aerogel material for building insulation, *Journal of Building Engineering*, 2021,
22 **44**, 102988.
- 23 17 J. Pett-Ridge, S. Kuebbing, A. C. Mayer, S. Hovorka, H. Pilorgé, S. E. Baker, S. H. Pang, C. D.
24 Scown, K. K. Mayfield and A. A. Wong, *Roads to removal: options for carbon dioxide removal in*
25 *the United States*, Lawrence Livermore National Laboratory (LLNL), Livermore, CA (United States),
26 2023.
- 27 18 B. Hirel, T. Tétu, P. J. Lea and F. Dubois, Improving Nitrogen Use Efficiency in Crops for
28 Sustainable Agriculture, *Sustainability*, 2011, **3**, 1452–1485.
- 29 19 Argonne National Laboratory, *Greenhouse gases, Regulated Emissions, and Energy use in*
30 *Technologies (GREET)*, US Dept. of Energy, 2023.
- 31 20 G. Wernet, C. Bauer, B. Steubing, J. Reinhard, E. Moreno-Ruiz and B. Weidema, Theecoinvent
32 database version 3 (part I): overview and methodology, *Int J Life Cycle Assess*, 2016, **21**, 1218–1230.
- 33 21 National Renewable Energy Laboratory, *U.S. Life Cycle Inventory Database*, 2012.
- 34 22 S. Kane and S. A. Miller, Mass, enthalpy, and chemical-derived emission flows in mineral
35 processing, *Journal of Industrial Ecology*, 2024, **28**, 469–481.
- 36 23 F. C. Bond, Crushing & Grinding Calculations Part 1, *British Chemical Engineering*, 1961, **6**, 378–
37 385.
- 38 24 US Dept. of Energy Advanced Manufacturing Office, *Manufacturing Energy and Carbon Footprints*
39 *(2018 MECS)*, 2021.
- 40 25 N. L. Weiss, *Particle Characterization, Mineral Processing Handbook*, American Institute of Mining
41 and Metallurgy, 1985.
- 42 26 Wade A. Amos, *Report on Biomass Drying Technology*, National Renewable Energy Lab, 1998.
- 43 27 U.S. Environmental Protection Agency, *Greenhouse Gas Inventory Guidance Direct Emissions from*
44 *Stationary Combustion Sources*, 2016.
- 45 28 S. C. Davis and R. G. Boundy, *Transportation Energy Data Book*, Oak Ridge National Laboratory,
46 39th edn., 2021.
- 47 29 United States Geological Survey, 2019.

- 1 30 Seth Kane and Sabbie A. Miller, Mass, enthalpy, and chemical-derived emissions flows in mineral
2 processing, *Journal of Industrial Ecology*.
- 3 31 M. L. Marceau, M. A. Nisbet and M. G. VanGeem, *Life Cycle Inventory of Portland Cement*
4 *Concrete*, Portland Cement Association, 2007.
- 5 32 D. Harrison, A. Bloodworth, J. Eyre, P. Scott and M. MacFarlane, Utilisation of mineral waste: a
6 scoping study, *British Geological Survey*.
- 7 33 C. Mitchell, *Quarry Fines and Waste*, British Geological Survey, 2009.
- 8 34 NSF, *Product Category Rule for Environmental Product Declarations: PCR for Concrete.*, 2019.
- 9 35 D. N. Huntzinger and T. D. Eatmon, A life-cycle assessment of Portland cement manufacturing:
10 comparing the traditional process with alternative technologies, *Journal of Cleaner Production*, 2009,
11 **17**, 668–675.
- 12 36 N. V. Y. Scarlett, I. C. Madsen, L. M. D. Cranswick, T. Lwin, E. Groleau, G. Stephenson, M.
13 Aylmore and N. Agron-Olshina, Outcomes of the International Union of Crystallography
14 Commission on Powder Diffraction Round Robin on Quantitative Phase Analysis: samples 2, 3, 4,
15 synthetic bauxite, natural granodiorite and pharmaceuticals, *J Appl Cryst*, 2002, **35**, 383–400.
- 16 37 S. Kaufhold, M. Hein, R. Dohrmann and K. Ufer, Quantification of the mineralogical composition of
17 clays using FTIR spectroscopy, *Vibrational Spectroscopy*, 2012, **59**, 29–39.
- 18 38 J. Karni and E. Karni, Gypsum in construction: origin and properties, *Materials and Structures*, 1995,
19 **28**, 92–100.
- 20 39 Lu, Liming, *Iron Ore - Mineralogy, Processing and Environmental Sustainability*, Elsevier, 2nd edn.,
21 2021.
- 22 40 P. Šiler, I. Kolářová, J. Bednárek, M. Janča, P. Musil and T. Opravil, The possibilities of analysis of
23 limestone chemical composition, *IOP Conf. Ser.: Mater. Sci. Eng.*, 2018, **379**, 012033.
- 24 41 F. Vegliò, B. Passariello and C. Abbruzzese, Iron Removal Process for High-Purity Silica Sands
25 Production by Oxalic Acid Leaching, *Ind. Eng. Chem. Res.*, 1999, **38**, 4443–4448.
- 26 42 A. Kim, P. R. Cunningham, K. Kamau-Devers and S. A. Miller, OpenConcrete: a tool for estimating
27 the environmental impacts from concrete production, *Environ. Res.: Infrastruct. Sustain.*, 2022, **2**,
28 041001.
- 29 43 J. Li, W. Zhang, C. Li and P. J. M. Monteiro, Eco-friendly mortar with high-volume diatomite and fly
30 ash: Performance and life-cycle assessment with regional variability, *Journal of Cleaner Production*,
31 2020, **261**, 121224.
- 32 44 American National Standards Institute, 2020.
- 33 45 P. D. Miles and W. B. Smith, Specific gravity and other properties of wood and bark for 156 tree
34 species found in North America, *Res. Note NRS-38. Newtown Square, PA: U.S. Department of*
35 *Agriculture, Forest Service, Northern Research Station. 35 p.*, 2009, **38**, 1–35.
- 36 46 C. D. Scown, A. A. Gokhale, P. A. Willems, A. Horvath and T. E. McKone, Role of Lignin in
37 Reducing Life-Cycle Carbon Emissions, Water Use, and Cost for United States Cellulosic Biofuels,
38 *Environ. Sci. Technol.*, 2014, **48**, 8446–8455.
- 39 47 N. R. Baral, O. Kavvada, D. Mendez Perez, A. Mukhopadhyay, T. S. Lee, B. A. Simmons and C. D.
40 Scown, Greenhouse Gas Footprint, Water-Intensity, and Production Cost of Bio-Based Isopentenol as
41 a Renewable Transportation Fuel, *ACS Sustainable Chem. Eng.*, 2019, **7**, 15434–15444.
- 42 48 B. Neupane, N. V. S. N. M. Konda, S. Singh, B. A. Simmons and C. D. Scown, Life-Cycle
43 Greenhouse Gas and Water Intensity of Cellulosic Biofuel Production Using Cholinium Lysinate
44 Ionic Liquid Pretreatment, *ACS Sustainable Chem. Eng.*, 2017, **5**, 10176–10185.
- 45 49 H. M. Breunig, J. Amirebrahimi, S. Smith and C. D. Scown, Role of Digestate and Biochar in
46 Carbon-Negative Bioenergy, *Environ. Sci. Technol.*, 2019, **53**, 12989–12998.
- 47 50 S. L. Nordahl, J. P. Devkota, J. Amirebrahimi, S. J. Smith, H. M. Breunig, C. V. Preble, A. J.
48 Satchwell, L. Jin, N. J. Brown, T. W. Kirchstetter and C. D. Scown, Life-Cycle Greenhouse Gas

1 Emissions and Human Health Trade-Offs of Organic Waste Management Strategies, *Environ. Sci.*
2 *Technol.*, 2020, **54**, 9200–9209.

3 51 S. L. Nordahl, N. R. Baral, B. A. Helms and C. D. Scown, Complementary roles for mechanical and
4 solvent-based recycling in low-carbon, circular polypropylene, *Proceedings of the National Academy*
5 *of Sciences*, 2023, **120**, e2306902120.

6 52 M. Puettmann, A. Sinha and I. Ganguly, Life Cycle Energy and Environmental Impacts of Cross
7 Laminated Timber Made with Coastal Douglas-fir, *Journal of Green Building*, 2019, **14**, 17–33.

8 53 K. Lan, S. S. Kelley, P. Nepal and Y. Yao, Dynamic life cycle carbon and energy analysis for cross-
9 laminated timber in the Southeastern United States, *Environmental Research Letters*, 2020, **15**,
10 124036.

11 54 M. Puettmann, A. Sinha and I. Ganguly, *CORRIM REPORT - Life Cycle Assessment of Cross*
12 *Laminated Timbers Produced in Oregon*, Consortium for Research on Renewable Industrial
13 Materials, 2017.

14 55 Athena Sustainable Materials Institute, *A Life Cycle Assessment of Cross-Laminated Timber*
15 *Produced in Canada*, Athena Sustainable Materials Institute, 2013.

16 56 M. Milota and M. E. Puettmann, Life-Cycle Assessment for the Cradle-to-Gate Production of
17 Softwood Lumber in the Pacific Northwest and Southeast Regions*, *Forest Products Journal*, 2017,
18 **67**, 331–342.

19 57 D. Abbas and R. M. Handler, Life-cycle assessment of forest harvesting and transportation operations
20 in Tennessee, *Journal of Cleaner Production*, 2018, **176**, 512–520.

21 58 S. S. Hubbard, R. D. Bergman, K. Sahoo and S. A. Bowe, A life cycle assessment of hardwood
22 lumber production in the northeast and north Central United States, *CORRIM Report. 45 p.*, 2020, 1–
23 45.

24 59 C. X. Chen, Environmental Assessment of the Production and End-of-Life of Cross-Laminated
25 Timber in Western Washington.

26 60 Portland Cement Association, *Environmental Product Declaration: Portland Cement*, 2021.

27 61 World Business Council For Sustainable Development, *The Cement Sustainability Initiative: Cement*
28 *Industry Energy and CO2 Performance, Getting the Numbers Right*, 2016.

29 62 Worldsteel association, *Life cycle inventory (LCI) study 2020 data release*, 2021.

30 63 International Energy Agency, *Iron and Steel Technology Roadmap – Analysis*, 2020.

31 64 G. J. Venta, *Life cycle analysis of gypsum board and associated finishing products*, ATHENATM
32 Sustainable Materials Institute, Ottawa, Canada, 1997.

33 65 Georgia-Pacific Gypsum LLC, *Type III environmental product declaration (EPD) for 1/2"*
34 *DensDeck® Prime Roof Board*, 2020.

35 66 Georgia-Pacific Gypsum LLC, *Type III environmental product declaration (EPD) for 1/2"*
36 *ToughRock® Mold-Guard™ Panel*, 2020.

37 67 Georgia-Pacific Gypsum LLC, *Type III environmental product declaration (EPD) for 1/2"*
38 *ToughRock® Lite-Weight Panel*, 2020.

39 68 Georgia-Pacific Gypsum LLC, *Type III environmental product declaration (EPD) for 1/2"*
40 *ToughRock® Fireguard C® Panel*, 2020.

41 69 Georgia-Pacific Gypsum LLC, *Type III environmental product declaration (EPD) for 1/2"*
42 *DensArmor Plus® C Panel*, 2020.

43 70 F. Pierobon, M. Huang, K. Simonen and I. Ganguly, Environmental benefits of using hybrid CLT
44 structure in midrise non-residential construction: An LCA based comparative case study in the U.S.
45 Pacific Northwest, *Journal of Building Engineering*, 2019, **26**, 100862.

46 71 Seth Kane and Sabbie A. Miller, A compositional, predictive model of biochar properties and
47 pyrolysis life-cycle inventories, *Bioresource Technology*.

- 1 72 S. Kane, A. Bin Thaneya, A. P. Gursel, J. Fan, B. Bose, T. P. Hendrickson, S. L. Nordahl, C. D.
2 Scown, S. A. Miller and A. Horvath, Uncertainty in carbon dioxide removal potential of biochar,
3 *Environmental Research Letters*.
- 4 73 A. Bin Thaneya, A. P. Gursel, S. Kane, S. A. Miller and A. Horvath, Assessing uncertainty in
5 building material emissions using scenario-aware Monte Carlo Simulation, *Environ. Res.: Infrastruct.*
6 *Sustain.*, DOI:10.1088/2634-4505/ad40ce.

7

Supplemental Information:
**A framework for ground-up life cycle assessment of novel, carbon-storing
building materials**

Seth Kane ^{a, †}, Baishakhi Bose ^b, Thomas P. Hendrickson ^c, Jin Fan ^a, Sarah L. Nordahl ^c,
Corinne D. Scown ^{b,c,d,e}, Sabbie A. Miller ^a

^a Department of Civil and Environmental Engineering, University of California, Davis

^b Biological Systems and Engineering Division, Lawrence Berkeley National Laboratory

^c Energy Analysis and Environmental Impacts Division, Lawrence Berkeley National Laboratory

^d Joint BioEnergy Institute, Lawrence Berkeley National Lab

^e Energy & Biosciences Institute, University of California, Berkeley

[†] Corresponding Author: T +1 907 750 6364, E skane@ucdavis.edu

1. Supplemental Introduction

In addition to the description of ordinary Portland cement and yellow poplar cross-laminated timber presented in the main text, additional mineral and biogenic materials were examined with the developed framework to provide additional examples of its application. For mineral-derived materials, these additional examples included the production of low-carbon steel and gypsum board. These materials represent the 2nd and 3rd most consumed, chemically processed mineral-derived materials in the US, and combined with cement, are responsible for 64% of total US chemically processed industrial minerals production.¹ In addition, they provide insight into applying this framework to meaningfully different processes than cement production and how this framework can provide increased insight into critical LCA decision-making for the treatment of drying, co-products, waste resources and feedstocks, and industrial symbiosis. In addition, we provide additional modeling details for biogenic resources, including example composition and carbon uptake data, and emission factors used for the analysis in the main text. While key results for these materials are given in the main text, here we provide complete model and process descriptions, as well as additional results.

2. Supplemental Methods

2.1 Biogenic material phases

Supplemental Table 1. Biomolecular composition across ten compounds for example biomass materials.

	Acetate	Ash	Cellulose	Hemicellulose	Lignin	Proteins	Butyric Acid	Extractive	Source
Sorghum	2.20%	4.00%	30.00%	20.70%	21.00%	4.39%	0.00%	17.71%	[4]
Corn stover	2.20%	5.77%	35.50%	25.31%	16.24%	3.70%	0.00%	11.28%	[5,6]
Miscanthus	0.50%	2.79%	41.42%	25.76%	21.41%	0.40%	7.72%	0.00%	[5,7]
Switchgrass	2.46%	3.45%	34.21%	21.54%	19.60%	4.88%	0.00%	13.86%	[4]
Pine	0.00%	0.07%	29.82%	13.48%	24.74%	0.00%	0.00%	31.89%	[8]
Walnut	0.00%	19.23%	26.29%	9.92%	17.63%	0.00%	0.00%	26.93%	[8]
Almond	0.00%	8.13%	38.54%	16.06%	21.63%	0.00%	0.00%	15.64%	[8]
Fir	0.00%	0.08%	28.46%	12.02%	23.42%	0.00%	0.00%	36.02%	[8]
Yellow Poplar	--	--	39.3%	18.4%	21.4%	--	--	--	[9]
Kraft Lignin (Eucalyptus)	--	--	1.7%	1.8%	98.2%	--	--	--	[10]
Kraft Lignin (Poplar)	--	--	1.3%	4.3%	91.0%	--	--	--	[10]
Kraft Lignin (Olive tree residue)	--	--	12.2%	10.3%	72.0%	--	--	--	[10]

Supplemental Table 2. Carbon content and carbon uptake for example biomass materials.

	Carbon Content (%)		Carbon Uptake (MT CO ₂ e/ha/yr)		Source
	Low	High	Low	High	
Sorghum	41.9%	44.6%	20.9	26	[11]
Corn stover	43.7%	44.8%	1.9	13.2	[12,13]
Miscanthus	44.6%	44.7%	36.2	42.2	[14]
Switchgrass	44.0%	45.7%	24.7	34.5	[11]
Pine	46.1%	48.2%	9.3	18.2	[15,16]
Walnut		46%	0.1	2.2	[17,18]
Almond		45%		5.9	[19,20]
Yellow Poplar	38.1%	43.5%	14.9	17.0	[21,22]
Fir	40.9%	49.1%	12.8	15.4	[23]
Lignin	60%	65%	N/A	N/A	[24]

2.1 Additional cement modeling details

Marl and cement rock calcium sources reported by the USGS as ~9% of total calcium sourcing are assumed to be primarily calcite and kaolinite and, therefore, are modeled as these two phases in limestone and kaolin. Silica (SiO₂) from silica sand, quartzite, and sandstone is used as the only silicon source. We note that numerous secondary silica sources (fly ash, steel slag, etc.) are reported by the USGS and are not included in this assessment. Both gibbsite (Al(OH)₃) and kaolinite (Al₂O₃·2SiO₂·2H₂O) are examined as aluminum sources. Kaolinite is obtained from kaolin clay (57.4% of aluminum) and shale (31.1% of aluminum). Gibbsite is examined from bauxite aluminum ores (11.4% of aluminum). Other aluminum-containing mineral phases in bauxite are not included in this analysis. The hematite (Fe₂O₃) phase in iron ore is modeled as the iron source. Other iron-containing phases were excluded.

Supplemental Table 3. Formation reactions of cement phases.

Cement phase	Wt. fraction	Raw mineral phase	Reaction	Phase production fraction
Alite	63%	Calcite, silica	$3\text{CaCO}_3 + \text{SiO}_2 \rightarrow \text{Ca}_3\text{SiO}_5 + 3\text{CO}_2$	100%
Belite	15%	Calcite, silica	$2\text{CaCO}_3 + \text{SiO}_2 \rightarrow \text{Ca}_2\text{SiO}_4 + 2\text{CO}_2$	100%
Aluminate	9%	Calcite, gibbsite	$3\text{CaCO}_3 + 2\text{Al}(\text{OH})_3 \rightarrow \text{Ca}_3\text{Al}_2\text{O}_6 + 3\text{CO}_2 + 3\text{H}_2\text{O}$	12.9%
		Calcite, kaolinite	$3\text{CaCO}_3 + \text{Al}_2\text{Si}_2\text{O}_5(\text{OH})_4 \rightarrow \text{Ca}_3\text{Al}_2\text{O}_6 + 3\text{CO}_2 + 2\text{SiO}_2 + 2\text{H}_2\text{O}$	87.1%
Ferrite	8%	Calcite, gibbsite, hematite	$4\text{CaCO}_3 + 2\text{Al}(\text{OH})_3 + \text{Fe}_2\text{O}_3 \rightarrow \text{Ca}_4\text{Al}_2\text{Fe}_2\text{O}_{10} + 4\text{CO}_2 + 3\text{H}_2\text{O}$	12.9%
		Calcite, kaolinite, hematite	$4\text{CaCO}_3 + \text{Al}_2\text{Si}_2\text{O}_5(\text{OH})_4 + \text{Fe}_2\text{O}_3 \rightarrow \text{Ca}_4\text{Al}_2\text{Fe}_2\text{O}_{10} + 4\text{CO}_2 + 2\text{H}_2\text{O} + 2\text{SiO}_2$	87.1%
Gypsum	5%	Gypsum	Used as mined.	65.5%
		Calcite	$\text{CaCO}_3 \rightarrow \text{CaO} + \text{CO}_2$; $\text{CaO} + \text{SO}_2 + 2\text{H}_2\text{O} + 0.5\text{O}_2 \rightarrow (\text{CaSO}_4 \cdot 2\text{H}_2\text{O})$	34.5%

As this mining LCI data included some crushing at the mine, an 80% passing particle size (F) for Bond's equation of 50,800 μm was used for all resources but silica sand (2,000 μm) and clay (2 μm). Ending 80% passing particle sizes (P) of 10 μm for all materials but clay (2 μm). For post-pyroprocessing milling, a starting size of 25,000 μm was used, and an ending size of 10 μm was used. Bond's Index values of 45.6 kJ/kg for limestone, 85.7 kJ/kg for silica sand, 28.6 kJ/kg for clay, 38.0 kJ/kg for Bauxite, 46.6 kJ/kg for iron ore, 26.2 kJ/kg for gypsum, and 51.9 kJ/kg for cement clinker were used.²

2.1 Steel process description

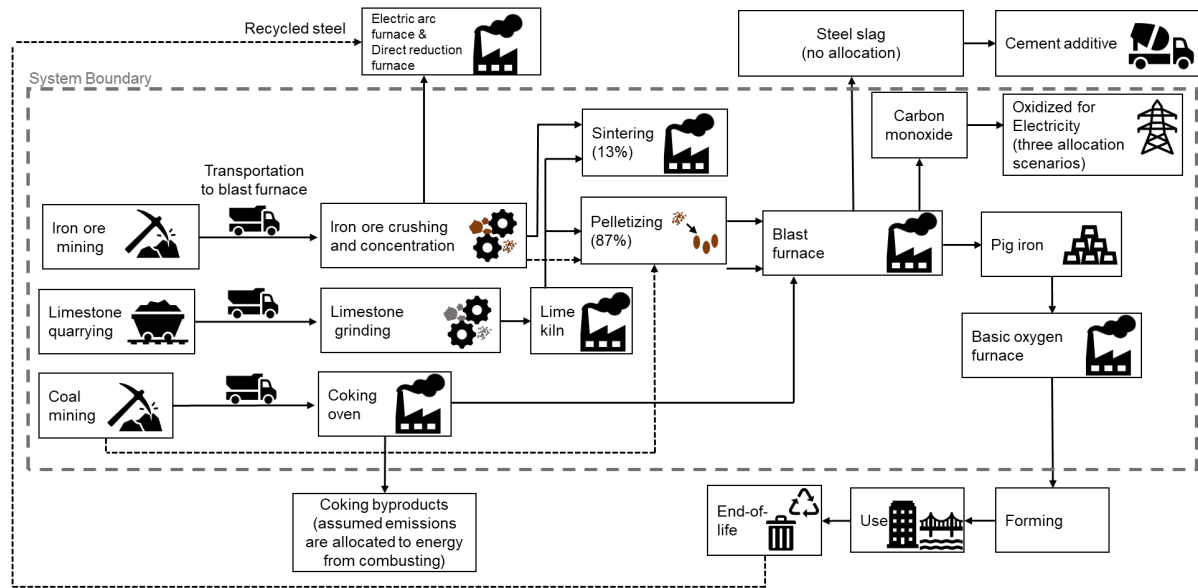
2.1.1 Scope

Low-carbon steel production is modeled as the average US primary production of direct-shipped iron ore, which requires no chemical beneficiation prior to sintering or pelletization.³ A blast furnace-basic oxygen furnace system is examined, as this is the predominant method of primary steel production in the US, comprising 96.5% of total domestic primary steel production as of 2019.⁴ The herein-used system boundary used to produce steel is shown in Supplemental Figure 1. The system is examined with a functional unit of 1 kg steel billet.

In the primary analysis, no allocation of emissions to the steel slag co-product is performed. In comparison with Worldsteel⁵ and International Energy Agency (IEA)⁶ steel emission values, we apply a system expansion approach to account for slag replacement of primary cement

production, using the emissions and energy for cement production as calculated in the main text. No allocation is performed to coking co-products – all emissions associated with potential downstream processing or use of these products are excluded. Three allocation scenarios are considered for energy produced from the combustion of blast furnace and basic oxygen furnace gas: (1) all emissions allocated to steel, (2) system expansion replacing primary electricity production (consistent with EIA modeling), and (3) all emissions allocated to energy.

Emissions associated with transportation are omitted, but past assessments have estimated energy use for transportation as 0.03 MJ/kg steel,⁵ or 0.2% of the herein calculated energy use. We do not assign emissions associated with the upstream processing of fuels, with the exception of stoichiometrically required metallurgical coke.



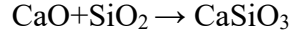
Supplemental Figure 1. System boundary to produce low-carbon steel.

2.1.2 Material composition and preparation

Iron ore composition is modeled as 63.72% Fe, 3.41% SiO₂, and 2.42% Al₂O₃,⁷ with iron present as 80% Fe₂O₃ (hematite) and 20% Fe₃O₄ (magnetite).¹ All moisture present in ores or added during beneficiation is assumed to be dried with waste heat. Prior to thermal processing, iron ore particle size is modeled as crushed at the mine to 50.8 mm and ground/milled to 2.59 mm for sintering and 50 μm for pelletizing. Energy inputs for crushing are accounted for in the mining inventories and grinding energy requirements are described with Bond's equation (see the main text). Other particle sizes before and after milling are bituminous coal for pelletizing 50.8 mm to 50 μm, anthracite coal for coking 50.8 mm to 25.4 mm, and limestone 50.8 mm to 125 μm, with the Bond's Index values described by Bond and in more recent studies.^{2,8}

2.1.3 Pelletizing, sintering, coking, and calcination reactions

Prior to the blast furnace, 13% of ore is sintered, while 87% is pelletized.⁴ Sintering is modeled with the following reactions:



26 wt.% of SiO₂ present in the iron ore (0.89 wt.% of total ore) is assumed to form CaSiO₃ during sintering,⁹ and 1.7 mol CaO is added per mol SiO₂ reacted during sintering.³ Sinter iron composition is modeled as 93 wt.% Fe₃O₄ and 7 wt.% Fe₂O₃. An energy efficiency of 26% is used for sintering,¹⁰ with an energy source of coke.

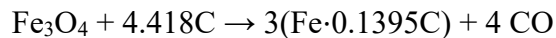
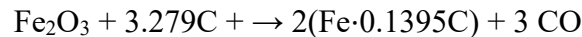
Pellets are modeled with a composition of 98 wt.% iron ore, 1 wt.% CaCO₃, and 1 wt.% anthracitic coal. Pelletizing energy requirements are met with the included anthracitic coal (emission factor of 0.0982 kg CO₂/MJ¹¹), with the remainder being met with blast furnace gas (emission factor of 0.26 kg CO₂/MJ¹¹).¹² Due to limited chemical reactions during pelletizing, the energy consumption during pelletizing is modeled directly as 0.5 MJ/kg steel,¹² excluding the energy produced by the combustion of coal inherent in pellets. This energy is primarily consumed for heating and phase transitions.

Pyrolysis of bituminous coal to form metallurgical coke is modeled based on previous experimentally determined enthalpies ($\Delta H_{\text{Rxn}} = 0.02651$ MJ/kg) and reactions (CO₂ emissions of 0.08586 kg/kg, and H₂O emissions of 0.860 kg/kg).^{1,13} Coke yields are modeled as 70% of initial coal inputs, and coke is assumed 86% carbon,¹⁴ with the remainder ash. The energy efficiency of coking is modeled as 51.2%, excluding energy recovery of flue gas co-products.¹⁵ Therefore, emissions associated with the combustion of coking flue gas co-products are assumed to be allocated to energy produced by the combustion of those products and are excluded. Fuel inputs to coking ovens are modeled as a mixture of coking byproduct gas and blast furnace gas, with the composition previously reported.¹⁵ This mixed gas has a LHV of 3.161 MJ/kg and CO₂ emissions of 0.18 kg CO₂/MJ, assuming complete combustion.

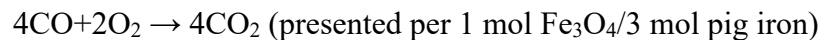
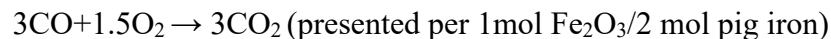
Limestone is used as the lime feedstock, and is calcined to form lime (CaO), with a thermal efficiency of 54.05%, and a fuel source of natural gas.

2.1.4 Blast furnace and basic-oxygen furnace reactions

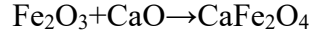
Reactions in the blast furnace are modeled based on the stoichiometric minimum carbon and oxygen content, with the assumption that pig iron is 3 wt.% C:¹



With the combustion of blast furnace gas to produce electricity:



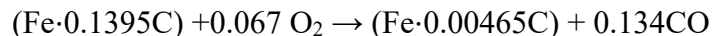
Slagging is modeled with lime added to reach a 1.7 CaO/SiO₂ molar ratio, with the assumption that all excess CaO reacts with Fe₂O₃ to form CaFe₂O₄ with the equation:



Lime reacts with SiO_2 with the same reaction as during sintering. Alumina present in iron ore and slag is modeled as non-reactive. Other reactions, including the reaction of phosphorus, manganese, and sulfur into slag, are excluded, due to their lower and highly variable content in iron ore. All blast furnace reactions are modeled with an energy efficiency of 39.13%,¹⁶ with a fuel source of 89% metallurgical coke, 7% electricity (at US average emission factor), and 4% natural gas.¹⁷ The energy efficiency of the oxidation of carbon monoxide to produce electricity is modeled as 37%.⁶

Reduction of hematite and magnetite to pig iron and carbon monoxide is endothermic ($\Delta H_{\text{Rxn}} = 247.25$ and 225 kJ/mol pig iron for hematite and magnetite, respectively). However, when including the oxidation of carbon monoxide to carbon dioxide, the entire process is net exothermic ($\Delta H_{\text{Rxn}} = -177.25$ and -152.333 kJ/mol pig iron for hematite and magnetite, respectively). Herein, we assign efficiency factors to both the endothermic and exothermic portions separately. Oxidation of carbon monoxide is assumed to replace primary electricity production, consistent with assumptions previously made by the IEA.⁶ Here, we examine three allocation scenarios for CO_2 emissions associated with the oxidation of carbon monoxide to the energy product: (1) all oxidation emissions allocated to low-carbon steel, (2) system expansion to include equivalent primary electricity production, and (3) all oxidation emissions allocated to electricity. We note that in Scenario 2, the emissions of steel are therefore dependent on the electricity grid and the specific location. For example, if the energy co-product of steel production were replacing a coal-heavy electric grid, steel production would be assigned lower emissions. If the energy co-product were replacing a low-carbon renewable energy grid, the emissions allocated to steel would be higher.

Basic oxygen furnaces were used to convert pig iron produced in the blast furnace to low-carbon steel, by reducing the carbon content from 3 wt.% to 0.1 wt.% with the reactions:



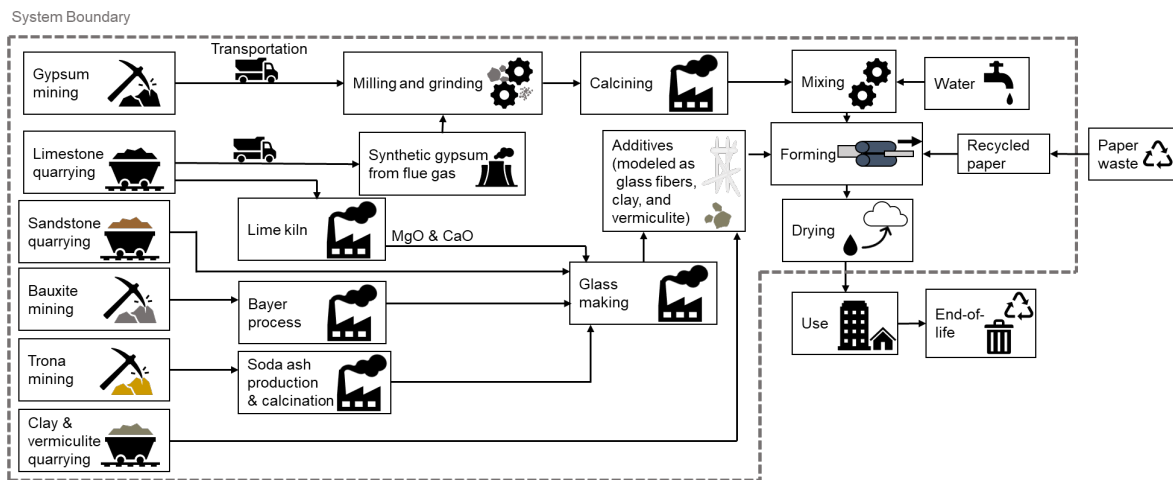
This reaction is exothermic and is assumed to follow immediately after the blast furnace, requiring no additional energy inputs. Oxidation of CO to CO_2 is modeled as described for the blast furnace, with the same allocation scenarios considered.

Facility overhead was determined based on the values reported by the *MECS*¹⁷ and normalized to per kg of material based on the US steel production reported by the USGS Mineral Yearbook.⁴ We note that this value also includes overhead for electric arc furnace and recycled steel production pathways, due to a lack of more granular data. This results in overhead energy consumption of 0.169 MJ/kg of low-carbon steel electricity and 0.795 MJ/kg of thermal and steam energy. We assume electricity is met at the US energy grid average emission factor, and thermal energy is met with the steel industry average of fuel resources, as reported by *MECS*.

2.2 Gypsum board process description

2.2.1 Scope

Production of gypsum board is modeled herein as regular type, 1/2 inch thickness, as this is the most produced gypsum board type in the US, at 95% of regular type production and 50% of all gypsum board production.⁴ Other thicknesses of regular gypsum board (5/8 inch) or types (e.g., type X) gypsum board are excluded from this analysis.¹⁸ The process flows and the system boundary used for the LCI of the regular gypsum board shown in Supplemental Figure 2. Paper in the gypsum board manufacturing process was modeled as recycled paper and was modeled with the same approach as mineral resources, as the chemical reaction approach can be applied to model the recycling process. The framework could be adapted to also apply the biogenic approach if primary paper was produced for use in gypsum board or could be extended to other types of gypsum board. A functional unit of 1 kg of gypsum board was used.



Supplemental Figure 2. System boundary and process flow diagram to produce gypsum board.

2.2.2 Gypsum board composition

Gypsum board typically contains mined gypsum ($\text{CaSO}_4 \cdot 2\text{H}_2\text{O}$), synthetic gypsum ($\text{CaSO}_4 \cdot 2\text{H}_2\text{O}$), vermiculite, clay, glass, and paper.¹⁹ The ratio of these mineral phases may vary depending on the type and thickness of gypsum board but is modeled herein with ratios typical of a regular type (1/2 inch) of gypsum board (89% gypsum, 5% paper, 2% vermiculite, 2% clay, 2% glass).²⁰ A ratio of 65.5% mined gypsum to 34.5% synthetic gypsum is used, based on ratios of total US gypsum consumption.⁴ The compositions of glass fibers were modeled based on a composition of 70% silica, 15% sodium oxide, 10% lime, 5% magnesium oxide, and 1% alumina.

2.2.3 Gypsum board formation

The formation of each phase in gypsum board was modeled with calcination and sulphuration reactions to form synthetic gypsum and calcining reactions prior to gypsum mixing and forming (Table 1).¹⁸ Vermiculite and clay were modeled as being used as quarried, and paper was modeled as recycled, which comprises ~100% of US gypsum board production.^{18,19} Glass production was modeled with previously described formation reactions.^{1,3}

The intermediate calcination of gypsum is modeled to account for the consumption of water and energy, with the assumption that neither heat nor water is recycled. The process involving mined gypsum is represented in two distinct reaction steps. The first step, as detailed in Table 1, involves the emission of H₂O; typically, this chemically-derived water is not recycled. Therefore, the water and energy consumption are modeled in the second reaction step of the gypsum synthesis process. Similarly, the process of using synthetic gypsum to produce gypsum board involves four steps. First, lime is produced from calcite and used in flue gas desulphurisation (FGD), as shown in Table 1. The following two steps of producing gypsum board from synthetic gypsum are modeled as the same as the mined gypsum process. The water and energy consumption are modeled in the second and third steps.

Supplemental Table 4. Formation reactions of gypsum board phases.

Gypsum board phase	Weight fraction	Raw mineral phase	Reaction	Phase production fraction
Gypsum	89%	Gypsum (mined)	$\text{CaSO}_4 \cdot 2\text{H}_2\text{O} \rightarrow (\text{CaSO}_4 \cdot 0.5\text{H}_2\text{O}) + 1.5\text{H}_2\text{O}$	65.5%
		Calcite (synthetic gypsum)	$\text{CaCO}_3 \rightarrow \text{CaO} + \text{CO}_2;$ $\text{CaO} + \text{SO}_2 + 2\text{H}_2\text{O} + 0.5\text{O}_2 \rightarrow (\text{CaSO}_4 \cdot 2\text{H}_2\text{O})$	34.5%
		Gypsum anhydrite	$(\text{CaSO}_4 \cdot 0.5\text{H}_2\text{O}) + 1.5\text{H}_2\text{O} \rightarrow \text{CaSO}_4 \cdot 2\text{H}_2\text{O}$	100%
Paper	5%	Paper	Used as recycled	100.0%
Vermiculite	2%	Vermiculite	No chemical processing	100.0%
Clay	2%	Clay	No chemical processing	100.0%
Glass	2%	Trona	US LCI data used.	100%

2.2.4 Processing of raw materials for gypsum board

Mineral composition was determined based on previously reported mineralogy of limestone, silica sand, bauxite, salt rock, trona, magnesite, and gypsum resources. Many of the resources used in the production of gypsum board are high purity, such as limestone at 98% calcite,²¹ silica sand at 99% silica,²² and gypsum at 92% gypsum.²³ In contrast, trona (82.4% trona),²⁴ bauxite

(53.17% gibbsite)²⁵ are typically less pure and therefore require more raw material relative to their stoichiometric requirement. Impurities in paper recycling were not considered, and both clay and vermiculite are typically used as mined. LCIs for all mining processes are from the US Lifecycle inventory database.²⁶

2.2.5 Material manufacture and assembly for gypsum board

The pyroprocessing efficiency is assumed to be 35.3% based on previous data from case studies.^{27,28} Glass fiber CO₂ emissions and energy use were determined from US LCI data.²⁹ The energy used in both gypsum calcining and post-forming drying is assumed to be met with natural gas. Lime production as a feedstock for synthetic gypsum production is modeled as 41.89% thermally efficient, with natural gas as the fuel source.

Material losses due to dust, spillage, and other sources were modeled with the same assumptions as in the Portland cement example for the mining (3%), milling and grinding (3%), pyroprocessing (3%), post-processing (3%), storage (1%), and transportation (3%) steps of the production process. As losses are applied multiplicatively, material losses downstream of the pyroprocessing step result in a net increase in mass flow through the high-emission and energy-requiring pyroprocessing step by 7.15%.

The transportation distances between gypsum quarries and gypsum board production facilities are often considered negligible,³⁰ as facilities are located near gypsum quarries, and relatively small amounts of other minerals are used. Similarly, the transport distances for synthetic gypsum production from quarries to flue-gas desulfurization locations have been considered negligible.³⁰ Facility overhead values of HVAC (0.01 MJ/kg gypsum board) and facility lighting (0.01 MJ/kg gypsum board) are assumed to be the same as those of Portland cement, due to a lack of reported data. Overhead energy consumption for packing and storage (0.04 MJ/kg gypsum board) and onsite transportation (0.03 MJ/kg gypsum board) are used based on previously reported energy consumption.²⁷

2.3 Additional methodology for biogenic materials

Supplemental Table 5: Life cycle inventory inputs for each stage of processing to produce 1 m³ of CLT.

Processing Stage	Input Parameter	Unit	YP	EH	Notes
Harvesting Operations	Equipment	kg	0.36*	0.33*	*include both use and maintenance
	Gasoline	MJ	24	19	
	Diesel	MJ	175	151	
	Lubricant	kg	0.3	0.2	
Sawmill Operations	Coal	MJ	–	734	
	Natural Gas	MJ	602	181	
	Gasoline	MJ	20.0	–	

	Diesel	MJ	198	–	
	Oil	MJ	0.7	268.5	
	Wood	MJ	1069.4*	3899*	*residues from sawmill operations
CLT Mill	Resin	kg	5.9	5.5	
	Electricity	kWh	118	111	
	Natural Gas	MJ	92	86	
Transportation to Sawmill	Flat Bed Truck	km	50	50	
	Logs Transported	mt	0.87	0.81	
Transportation to CLT Mill	Flat Bed Truck	km	61.2	61.2	
	Logs Transported	mt	0.52	0.48	

Supplemental Table 6: Life-cycle GHG intensities for the life cycle inventory inputs used in this study.

Parameter	Life-Cycle Emission Factor					References
	CH ₄	NO ₂	CO ₂	CO _{2e}	Unit [†]	
Equipment	--	--	--	46.6	kg/dry ton wood	³¹
Gasoline*	1.4E-04	8.0E-07	1.0E-01	--	kg/MJ	Upstream emissions calculated using AgileC2G and data from Nordahl <i>et al.</i> 2023. ³² Combustion emissions are calculated using data from the US EPA. ³³
Coal*	1.6E-04	1.5E-06	9.4E-02	--	kg/MJ	
Oil*	9.2E-05	6.2E-07	7.7E-02	--	kg/MJ	
Natural Gas*	1.1E-04	3.3E-08	5.9E-02	--	kg/MJ	Upstream and combustion emissions calculated using AgileC2G and data from Nordahl <i>et al.</i> 2023. ³²
Diesel*	1.1E-04	1.1E-06	9.3E-02	--	kg/MJ	
Lubricant	4.9E-04	2.7E-06	1.9E-01	--	kg/kg	³¹
Wood	9.6E-03	4.2E-03	--	--	kg/kg	³⁴
Resin	2.1E-03	1.8E-04	5.6E-01	--	kg/kg	³¹
Electricity	1.4E-05	2.1E-04	2.3E-01	--	kg/KWh	³³
Flat Bed Truck	2.7E-04	6.4E-07	2.1E-01	--	kg/Mt-km	³¹

*Includes both upstream emissions and combustion emissions.

3. Supplemental Results

Material composition was determined based on previously reported mineralogy of limestone, silica sand, bauxite, clay, ferrous ore, and gypsum resources. Many of the resources used in the production of Portland cement are high purity, such as limestone at 98% calcite²¹, silica sand at 99% silica²², and gypsum at 92% gypsum.²³ In contrast, bauxite (53.17% gibbsite²⁵), clay (41% kaolinite³⁵), and ferrous ore (64% hematite³⁶) are typically less pure and therefore require more raw material relative to their

stoichiometric requirement (Main text Figure 5a). We note that we do not account for impurities that could replace other primary resources. For example, reasonable quantities of silica are present in both clay (8%) and bauxite (6.3%). Unaccounted-for impurities may increase energy consumption associated with mining, grinding, and milling processing steps, but given the high uncertainty and spatial variability in mineral composition, not accounting for these impurities provides a conservative estimate for the energy requirement of these processes.

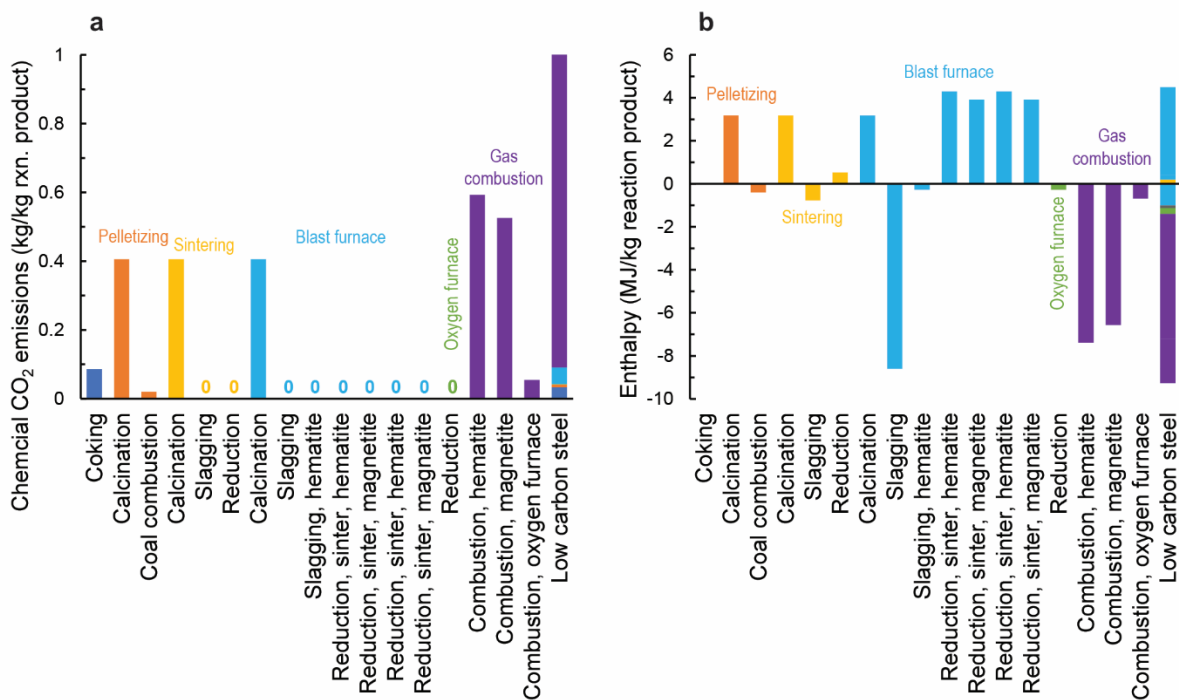
3.1 Steelmaking

Mineral feedstocks in steelmaking are dominated by inputs of ferrous ore (1.555 kg/kg steel), and bituminous coal for coking (0.581 kg/kg steel), in addition to a small portion of limestone (0.129 kg/kg steel, Supplemental Figure 3). In total, 2.25 kg of mineral inputs are required to produce 1 kg of steel, excluding material waste during processing. When including material waste after the mine, an additional 0.28 kg of minerals are consumed, resulting in 2.53 kg total mineral resource consumption per kg of steel.

When comparing the three allocation scenarios, the allocation of all furnace gas emissions to electricity reduces the GHG emissions of steel by 45% compared to allocating all emissions to steel. The scenario where system expansion to include US grid average electricity production is used to account for the additional energy production results in a reduction of 11.6% relative to all emissions allocated to steel. As energy consumed and produced were accounted for separately, no changes in energy consumption occurred in any allocation scenarios.

Similarly, the endothermic enthalpy requirement of steelmaking is predominantly driven by the blast furnace processing step, at 78% of the total of 4.5 MJ/kg steel required enthalpy. Exothermic reactions, primarily due to combustion of blast furnace and oxygen furnace gas release 9.3 MJ/kg steel enthalpy. Due to their small mass contributions, endothermic enthalpy contributions of calcination reactions and exothermic contributions of slagging reactions are relatively small, comprising 5% and 12% of the total endothermic and exothermic enthalpy, respectively.

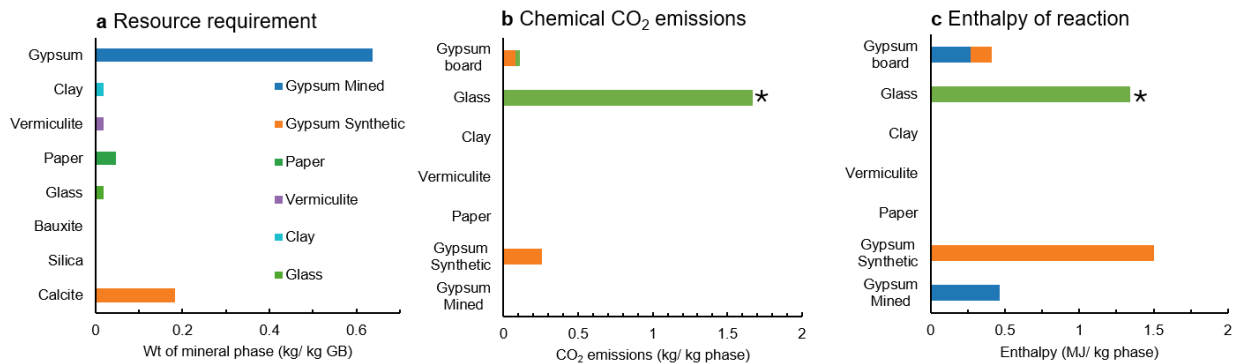
Blast furnace processing, efficiency data, and conversion of blast furnace gas to energy all have broadly reported and high-quality underlying data. In contrast, other processing, such as pelletizing and sintering, show higher variation between sources for underlying data, such as process efficiency, and mining may have variations due to ore composition. However, as these processes make up small fractions of the total GHG emissions, the result is relatively insensitive to variations in emissions associated with these processes. Compared to Portland cement, overhead energy consumption used for factors such as facility HVAC, lighting, and onsite transportation makes up a relatively high fraction of both emissions and energy consumption, at 7.1% of energy consumption and 3.4% of GHG emissions when all emissions are allocated to steel.



Supplemental Figure 3. (a) Chemically-derived CO₂ emissions and (b) enthalpy of reaction for steel-making reactions. Values are shown for 1 kg of reaction primary product, except the totaled low-carbon steel, which is a summation for 1 kg of low-carbon steel. No allocation of energy products from the combustion of blast or oxygen furnaces was performed at this stage of calculations.

When all emissions are allocated to steel, steelmaking emits 2.854 kg CO₂ / kg steel, driven largely by chemical emissions from the combustion of blast furnace and oxygen furnace gas. Energy emissions due to blast furnace enthalpy and inefficiency energy consumption make up the majority of remaining emissions, and combined, these three categories comprise 85% of total CO₂ emissions. We note that this is an area where data used in this assessment has a higher degree of certainty, blast furnace processing, efficiency data, and conversion of blast furnace gas to energy all have broadly reported and high-quality underlying data. In contrast, other processing, such as pelletizing and sintering, show higher variation between sources for underlying data such as process efficiency, and mining may have variations due to ore type. However, as these processes make up small fractions of the total CO₂ emissions, the result is relatively insensitive to variations in emissions associated with these processes. Compared to Portland cement, overhead energy consumption used for factors such as facility HVAC, lighting, and onsite transportation makes up a relatively high fraction of both emissions and energy consumption, at 7.1% of energy consumption and 3.4% of CO₂ emissions when all emissions are allocated to steel.

3.2 Gypsum board production



Supplemental Figure 4. First principle values for the chemical conversion of raw resources into cement, including: (a) mineral mass input requirement for 1 kg gypsum board, (b) chemically-derived CO₂ emissions, and (c) energy required by the enthalpy of reaction. Results in (b) and (c) are displayed for 1 kg of each material constituent. *Glass enthalpy and chemical CO₂ emissions are shown for reference; existing LCI data are used for glass fibers.

Production of 1 mol synthetic gypsum, one of the primary mineral phases in gypsum board, results in 1 mol CO₂ for a mass ratio of 0.26 kg CO₂ / kg synthetic gypsum. However, as gypsum production relies heavily on natural gypsum, which has no associated chemically-derived emissions, the total resulting chemically-derived emissions for gypsum board is 0.084 kg CO₂ / kg gypsum board. Notably, however, production of synthetic gypsum also sequesters 1 mol of SO₂ per mol of synthetic gypsum produced, typically from coal flues or metallurgical roasting reactions, such as those used in copper production. Despite relatively large emissions for the glass fibers on a mass basis (1.67 kg CO₂ / kg glass fiber), they have only a minor contribution to the emissions of gypsum board (0.032 kg CO₂ / kg gypsum board), due to their low mass fraction.

Similarly, the enthalpy of reaction to produce gypsum board is 0.73 MJ / kg gypsum board, due to the dehydration of gypsum (Supplemental Figure 4c) as it has both notable enthalpy of formation and it is the phase present in the greatest quantity. Per kg of each phase, glass has the largest contribution to the required enthalpy of formation for gypsum board at 1.34 MJ / kg glass. We note that the exothermic enthalpy of reaction of synthetic gypsum was treated as zero, assuming that the heat in this process was not reused. However, the framework could be adapted to a case where heat present in flue gas is used, and appropriate allocation applied as in the low-carbon steel example.

As a result of mineral impurities and mass loss due to material waste and chemically derived emissions, a total mass of 0.94 kg raw material is required per kg gypsum board, exclusive of water (Main text Figure 7b) The extracted mineral is smaller than 1 kg because the production of synthetic gypsum involves a reaction with gas phase SO₂, which is not accounted for in the raw material requirement. Extraction of these resources consumes 1.37 MJ / kg gypsum board, with this energy being primarily natural gas, electricity, and diesel consumption in paper recycling (0.82 MJ / kg gypsum board). Grinding and milling processes of gypsum prior to calcination result in an energy consumption of 0.03 MJ / kg gypsum board. After adding excessive water in

the post-milling process to make gypsum mixture, the re-drying consumed significant energy of 1.82 MJ/kg gypsum board. It is worth noting that this additional step of adding water beyond the chemical requirement to reduce viscosity prior to forming, and then evaporation of this water in the manufacturing process is associated with significant energy consumption and CO₂ emissions. Water consumption shown in Main Text Figure 7b only accounts for the chemically required water to produce gypsum powder, which did not include the excessive water added at the gypsum board manufacturing stage.

In contrast to the Portland cement and low-carbon steel examples, the energy consumption of gypsum board production is dominated by the post-processing, which consumes 33% of the total energy (Main Text Figure 8b). The post-processing energy consumption is primarily for re-drying the gypsum mixture to remove excessive water that was introduced during mixing steps. Paper recycling in the raw material extraction stage plays the next largest role in energy consumption, at 60% of raw material extraction energy consumption, and 15% of total energy consumption, respectively. CO₂ emissions from the production of gypsum board are dominated by mineral extraction (25%) and followed by post-processing (23%). The total CO₂ emissions resulted from material extraction were primarily driven by the energy intensity of paper recycling. With 19% of total CO₂ emissions resulting from chemically-derived emissions from chemical conversion, primarily due to the production of synthetic gypsum. About 3% of total CO₂ emissions result from energy consumption for the pre-milling and grinding of mineral resources.

The total energy consumed to produce 1 kg of gypsum board was modeled as 5.46 MJ, which is in the range of previously reported energy use of 3.44-6.74 MJ/kg gypsum board.^{18,20,37-40} Transportation of raw materials contributes to ~5% of total emissions,³⁰ which were excluded in this study. In addition, the variation of kiln efficiency, paper recycling technologies, and the use of excess water that needs to be evaporated could also cause the discrepancy. The GHG emissions determined herein are in good agreement with other analyses of the gypsum board industry. For example, GHGs reported in several 1/2 inch gypsum boards are in a range of 0.30-0.48 kg CO₂-eq / kg gypsum board,^{18,20,37-40} which shows good agreement with our proposed method of 0.44 kg CO₂-eq / kg gypsum board.

Supplemental References

- (1) Kane, S.; Miller, S. A. Mass, Enthalpy, and Chemical-Derived Emission Flows in Mineral Processing. *J. Ind. Ecol.* n/a (n/a). <https://doi.org/10.1111/jiec.13476>.
- (2) Bond, F. C. Crushing & Grinding Calculations Part 1. *Br. Chem. Eng.* **1961**, *6*, 378–385.
- (3) Ullmann's Encyclopedia of Industrial Chemistry. *Ullmanns Encycl. Ind. Chem.* **2000**. <https://doi.org/10.1002/14356007>.
- (4) United States Geological Survey. Minerals Yearbook - Metals and Minerals, 2019.
- (5) Worldsteel association. *Life Cycle Inventory (LCI) Study 2020 Data Release*; 2021. <https://worldsteel.org/wp-content/uploads/Life-cycle-inventory-LCI-study-2020-data-release.pdf>.
- (6) International Energy Agency. *Iron and Steel Technology Roadmap – Analysis*; 2020. <https://www.iea.org/reports/iron-and-steel-technology-roadmap> (accessed 2024-06-20).

- (7) Umadevi, T.; Sampath Kumar, M. G.; Mahapatra, P. C.; Mohan Babu, T.; Ranjan, M. Recycling of Steel Plant Mill Scale via Iron Ore Pelletisation Process. *Ironmak. Steelmak.* **2009**, *36* (6), 409–415. <https://doi.org/10.1179/174328108X393795>.
- (8) de Bakker, J. Energy Use of Fine Grinding in Mineral Processing. *Metall. Mater. Trans. E* **2014**, *1* (1), 8–19. <https://doi.org/10.1007/s40553-013-0001-6>.
- (9) Iosif, A.-M.; Hanrot, F.; Ablitzer, D. Process Integrated Modelling for Steelmaking Life Cycle Inventory Analysis. *Environ. Impact Assess. Rev.* **2008**, *28* (7), 429–438. <https://doi.org/10.1016/j.eiar.2007.10.003>.
- (10) Azevedo, J. M. C.; CabreraSerrenho, A.; Allwood, J. M. Energy and Material Efficiency of Steel Powder Metallurgy. *Powder Technol.* **2018**, *328*, 329–336. <https://doi.org/10.1016/j.powtec.2018.01.009>.
- (11) U.S. Environmental Protection Agency. *Greenhouse Gas Inventory Guidance Direct Emissions from Stationary Combustion Sources*; 2016. https://www.epa.gov/sites/default/files/2016-03/documents/stationaryemissions_3_2016.pdf.
- (12) Lv, W.; Sun, Z.; Su, Z. Life Cycle Energy Consumption and Greenhouse Gas Emissions of Iron Pelletizing Process in China, a Case Study. *J. Clean. Prod.* **2019**, *233*, 1314–1321. <https://doi.org/10.1016/j.jclepro.2019.06.180>.
- (13) Jacob, K. T.; Seetharaman, S. Thermodynamic Stability of Metallurgical Coke Relative to Graphite. *Metall. Mater. Trans. B* **1994**, *25* (1), 149–151. <https://doi.org/10.1007/BF02663188>.
- (14) Schobert, H.; Schobert, N. Comparative Carbon Footprints of Metallurgical Coke and Anthracite for Blast Furnace and Electric Arc Furnace Use. Archival Report Prepared for Blaschak Coal Corp.
- (15) Ergul, M.; Selimli, S. An Applied Study on Energy Analysis of a Coke Oven. *Sci. Technol. Energy Transit.* **2024**, *79*, 1. <https://doi.org/10.2516/stet/2023042>.
- (16) Rasul, M. G.; Tanty, B. S.; Mohanty, B. Modelling and Analysis of Blast Furnace Performance for Efficient Utilization of Energy. *Appl. Therm. Eng.* **2007**, *27* (1), 78–88. <https://doi.org/10.1016/j.applthermaleng.2006.04.026>.
- (17) US Dept. of Energy Advanced Manufacturing Office. *Manufacturing Energy and Carbon Footprints (2018 MECS)*; 2021.
- (18) Venta, G. J. *Life Cycle Analysis of Gypsum Board and Associated Finishing Products*; ATHENATM Sustainable Materials Institute: Ottawa, Canada, 1997.
- (19) Lushnikova, N.; Dvorkin, L. 25 - Sustainability of Gypsum Products as a Construction Material. In *Sustainability of Construction Materials (Second Edition)*; Khatib, J. M., Ed.; Woodhead Publishing, 2016; pp 643–681. <https://doi.org/10.1016/B978-0-08-100370-1.00025-1>.
- (20) Georgia-Pacific Gypsum LLC. *Type III Environmental Product Declaration (EPD) for 1/2" ToughRock® Mold-Guard™ Panel*; EPD10310; 2020.
- (21) Šiler, P.; Kolářová, I.; Bednárek, J.; Janča, M.; Musil, P.; Opravil, T. The Possibilities of Analysis of Limestone Chemical Composition. *IOP Conf. Ser. Mater. Sci. Eng.* **2018**, *379* (1), 012033. <https://doi.org/10.1088/1757-899X/379/1/012033>.
- (22) Vegliò, F.; Passariello, B.; Abbruzzese, C. Iron Removal Process for High-Purity Silica Sands Production by Oxalic Acid Leaching. *Ind. Eng. Chem. Res.* **1999**, *38* (11), 4443–4448. <https://doi.org/10.1021/ie990156b>.

- (23) Karni, J.; Karni, E. Gypsum in Construction: Origin and Properties. *Mater. Struct.* **1995**, *28* (2), 92–100. <https://doi.org/10.1007/BF02473176>.
- (24) Wiig, S. V.; Grundy, W.; Dyni, J. R. *Trona Resources in the Green River Basin, Southwest Wyoming*; US Geological Survey, 1995.
- (25) Chen, Q.; Zeng, W. Calorimetric Determination of the Standard Enthalpies of Formation of Gibbsite, Al(OH)₃(Cr), and Boehmite, AlOOH(Cr). *Geochim. Cosmochim. Acta* **1996**, *60* (1), 1–5. [https://doi.org/10.1016/0016-7037\(95\)00378-9](https://doi.org/10.1016/0016-7037(95)00378-9).
- (26) National Renewable Energy Laboratory. *U.S. Life Cycle Inventory Database*; 2012. <https://www.lcacommons.gov/nrel/search>.
- (27) Pedreño-Rojas, M. A.; Fořt, J.; Černý, R.; Rubio-de-Hita, P. Life Cycle Assessment of Natural and Recycled Gypsum Production in the Spanish Context. *J. Clean. Prod.* **2020**, *253*, 120056. <https://doi.org/10.1016/j.jclepro.2020.120056>.
- (28) Suárez, S.; Roca, X.; Gasso, S. Product-Specific Life Cycle Assessment of Recycled Gypsum as a Replacement for Natural Gypsum in Ordinary Portland Cement: Application to the Spanish Context. *J. Clean. Prod.* **2016**, *117*, 150–159. <https://doi.org/10.1016/j.jclepro.2016.01.044>.
- (29) National Renewable Energy Laboratory. *United States Life Cycle Inventory Database*, 2012. <https://www.lcacommons.gov/nrel/search>.
- (30) Fořt, J.; Černý, R. Carbon Footprint Analysis of Calcined Gypsum Production in the Czech Republic. *J. Clean. Prod.* **2018**, *177*, 795–802. <https://doi.org/10.1016/j.jclepro.2018.01.002>.
- (31) Abbas, D.; Handler, R. M. Life-Cycle Assessment of Forest Harvesting and Transportation Operations in Tennessee. *J. Clean. Prod.* **2018**, *176*, 512–520. <https://doi.org/10.1016/j.jclepro.2017.11.238>.
- (32) Nordahl, S. L.; Baral, N. R.; Helms, B. A.; Scown, C. D. Complementary Roles for Mechanical and Solvent-Based Recycling in Low-Carbon, Circular Polypropylene. *Proc. Natl. Acad. Sci.* **2023**, *120* (46), e2306902120. <https://doi.org/10.1073/pnas.2306902120>.
- (33) United States Environmental Protection Agency. *Emissions & Generation Resource Integrated Database (eGRID)*, 2023. <https://www.epa.gov/egrid>.
- (34) Milota, M.; Puettmann, M. E. Life-Cycle Assessment for the Cradle-to-Gate Production of Softwood Lumber in the Pacific Northwest and Southeast Regions*. *For. Prod. J.* **2017**, *67* (5–6), 331–342. <https://doi.org/10.13073/FPJ-D-16-00062>.
- (35) Kaufhold, S.; Hein, M.; Dohrmann, R.; Ufer, K. Quantification of the Mineralogical Composition of Clays Using FTIR Spectroscopy. *Vib. Spectrosc.* **2012**, *59*, 29–39. <https://doi.org/10.1016/j.vibspec.2011.12.012>.
- (36) Lu, Liming. *Iron Ore - Mineralogy, Processing and Environmental Sustainability*, 2nd ed.; Elsevier, 2021.
- (37) Georgia-Pacific Gypsum LLC. *Type III Environmental Product Declaration (EPD) for 1/2" ToughRock® Fireguard C® Panel*; EPD10310; 2020.
- (38) Georgia-Pacific Gypsum LLC. *Type III Environmental Product Declaration (EPD) for 1/2" DensArmor Plus® C Panel*; EPD10310; 2020.
- (39) Georgia-Pacific Gypsum LLC. *Type III Environmental Product Declaration (EPD) for 1/2" ToughRock® Lite-Weight Panel*; EPD10310; 2020.
- (40) Georgia-Pacific Gypsum LLC. *Type III Environmental Product Declaration (EPD) for 1/2" DensDeck® Prime Roof Board*; EPD10310; 2020.